PL-TR-96-2306

ADVANCED GEOPHYSICAL ENVIRONMENT SIMULATION TECHNIQUES

G. B. Gustafson
R. P. d'Entremont
C. F. Ivaldi
S. T. Beresford
C. P. Sarkisian
D. B. Hogan

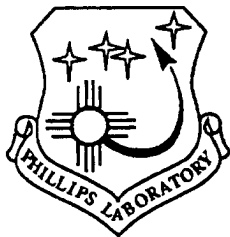Atmospheric and Environmental Research, Inc.
840 Memorial Drive
Cambridge, MA 02139

1 December 1996

Scientific Report No. 2

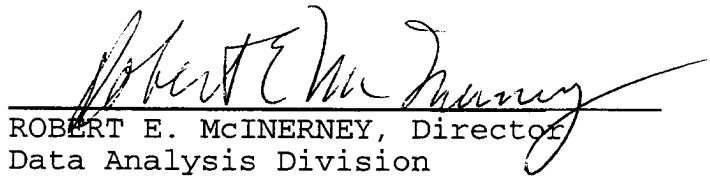Approved for public release; distribution unlimited

19971110 047

PHILLIPS LABORATORY
Directorate of Geophysics
AIR FORCE MATERIEL COMMAND
HANSCOM AIR FORCE BASE, MA 01731-3010

DTIC QUALITY INSPECTED 3

"This technical report has been reviewed and is approved for publication"

REPORT DOCUMENTATION PAGE

1. AGENCY USE ONLY *(Leave blank)*	2. REPORT DATE 1 December 1996	3. REPORT TYPE AND DATES COVERED Scientific Report No. 2

4. TITLE AND SUBTITLE

Advanced Geophysical Environment Simulation Techniques

5. FUNDING NUMBERS

PE 35160F
PR 7659 TA GY
WU AC
Contract:
F19628-94-C-0106

6. AUTHOR(S)

G. B. Gustafson   S. T. Beresford
R. P. d'Entremont   C. P. Sarkisian
C. F. Ivaldi   D. B. Hogan

7. PERFORMING ORGANIZATION NAME(S) AND ADDRESS(ES)

Atmospheric and Environmental Research, Inc.
840 Memorial Drive
Cambridge, MA 02139

8. PERFORMING ORGANIZATION REPORT NUMBER

9. SPONSORING/MONITORING AGENCY NAME(S) AND ADDRESS(ES)

Phillips Laboratory
29 Randolph Road
Hanscom AFB, MA 01731-3010
Contract Manager: Edward Robinson/GPD

10. SPONSORING/MONITORING AGENCY REPORT NUMBER

PL-TR-96-2306

11. SUPPLEMENTARY NOTES

12a. DISTRIBUTION/AVAILABILITY STATEMENT

Approved for public release;
distribution unlimited

12b. DISTRIBUTION CODE

13. ABSTRACT *(Maximum 200 words)*

This interim scientific report describes a multi-faceted effort to support PL/GPD in the development and application of state-of-the-art analysis techniques for remotely sensed data. The resulting tools, techniques and data sets will support the improved analysis of archived data as well as current and future geophysical parameter acquisition and analysis. The principal accomplishments during the reporting period were: development of improved algorithms for retrieval of cirrus emissivity and estimation of cloud altitude; development of improved cloud-phase discrimination algorithms for analysis of GOES imager and AVHRR data; application of existing cloud detection and new cloud-phase and emissivity algorithms to a two-month data set collected from one GOES and two NOAA satellites over the eastern and central portions of the continental U.S. and western Atlantic; reduction and quality assurance processing of approximately one month of raw radiosonde data from five sites; and software tool and technique development for enhanced satellite image processing capabilities on the Air Force Interactive Meteorological System.

14. SUBJECT TERMS

cirrus, optical properties, cloud altitude, data analysis
AIMS

15. NUMBER OF PAGES
56

16. PRICE CODE

17. SECURITY CLASSIFICATION OF REPORT Unclassified	18. SECURITY CLASSIFICATION OF THIS PAGE Unclassified	19. SECURITY CLASSIFICATION OF ABSTRACT Unclassified	20. LIMITATION OF ABSTRACT SAR

NSN 7540-01-280-5500

Standard Form 298 (Rev. 2-89)

TABLE OF CONTENTS

LIST OF FIGURES

LIST OF FIGURES (Continued)

LIST OF TABLES

1. INTRODUCTION AND OVERVIEW

This document describes a multi-faceted effort to support PL/GPD in the development and application of state-of-the-art analysis techniques for remotely sensed data. The resulting tools, techniques and data sets will support the improved analysis of archived data as well as current and future geophysical parameter acquisition and analysis. The principal accomplishments during the reporting period were:

- development of improved algorithms for retrieval of cirrus emissivity and estimation of cloud altitude;

- development of improved cloud-phase discrimination algorithms for analysis of GOES imager and AVHRR data;

- application of existing cloud detection and new cloud-phase and emissivity algorithms to a two-month data set collected from one GOES and two NOAA satellites over the eastern and central portions of the continental U.S. and western Atlantic;

- reduction and quality assurance processing of approximately one month of raw radiosonde data from five sites; and

- software tool and technique development for enhanced satellite image processing capabilities on the Air Force Interactive Meteorological System.

All software development and data processing were performed on the Air Force Interactive Meteorological System (AIMS) located at the Air Force Phillips Laboratory Atmospheric Sciences Division (PL/GPA) facility at Hanscom Air Force Base. AIMS is an integrated facility consisting of multiple real-time meteorological satellite receiving stations, a comprehensive archive of satellite and conventional data products, a powerful database access system, a rich set of state-of-the-art algorithms for satellite data analysis, and a mixed computing environment. It is operated jointly by the U.S. Air Force and Atmospheric and Environmental Research, Inc. (AER) under the terms of a Cooperative Research and Development Agreement (CRADA).

Cloud-analysis related algorithm development built on an existing set of satellite analysis algorithms developed under earlier programs at the Phillips Laboratory. The key research project codes are:

- TACNEPH (contract # F19628-90-C-0112): basic cloud properties (cover, layers, type) for DMSP and NOAA satellites as appropriate for processing in a military tactical environment;

- SERCAA Phase I (contract # F19628-92-C-0149): basic cloud properties (cover, layers, type) for both polar-orbiting (DMSP and NOAA series) and geosynchronous (GOES, GMS and METEOSAT) satellites plus a merge processing step which produces a best synoptic analysis from all available data;

- SERCAA Phase II (contract # F19628-92-C-0149): enhanced cloud properties including cirrus properties (emissivity, effective height and effective temperature), cloud phase, and integration of cloud analysis with microwave sounding.

1

Algorithm development and data analysis work was to support the Background Working Group of the of the Space Based Infrared System (SBIRS) Phenomenology Exploitation Project. Radiosonde data processing was in support of a Phillips Lab project to investigate conditions conducive to contrail formation. AIMS development is to improve the state of the art of satellite image analysis and visualization capabilities.

This remainder of this report is organized as follows. Section 2 summarizes the new cloud analysis algorithm development; Section 3 presents the work on the data set generation to support the SBIRS Phenomenology Exploitation Project; Section 4 presents the data reduction and quality assurance work on the radiosonde data collected for the contrail program; and Section 5 summarizes AIMS improvements.

2. CLOUD-PROPERTY RETRIEVAL ALGORITHM DEVELOPMENT

Transmissive cirrus clouds both emit and transmit thermal energy. Emissions occur at a rate dependent on cirrus emissivity and temperature, while transmissions depend most strongly on cirrus transmissivity and the temperature of the underlying warmer surface (either a lower cloud or the ground). Physical retrievals of cirrus radiative and spatial properties must account appropriately for these attributes. If the semi-transparent nature of cirrus clouds is not properly modeled, its altitude is consistently underestimated when using passive infrared brightness temperature data.

There are many sources of passive satellite data that can be used to detect and analyze cirrus attributes. Among the earliest are visible and infrared data of the 1960s from the TIROS series of polar orbiting satellites, augmented in the early 1970s by geostationary GOES data. More recent TIROS sensors include the Advanced Very High Resolution Radiometer (AVHRR), a five-channel passive radiometer with detectors that measure upwelling visible (0.63 μm), near-infrared (NIR, 0.86 μm), middle wavelength IR (MWIR, 3.7 μm), and split longwave IR (LWIR, 10.7 and 11.8 μm) energy both day and night. The sounder instruments collectively known as TOVS (TIROS Operational Vertical Sounder) also collect data in the wings of the 15-μm CO_2 absorption band that are useful for detection of thin cirrus and specification of their height. Current GOES-Next Imager and Sounder infrared channels useful for detection of cirrus include 3.9, 6.7, 11.2, 12.7 (Channels 2, 3, 4, and 5, respectively), and CO_2 13.3-14.5 μm spectral bands. GOES MWIR and LWIR imager data are 4-km resolution; AVHRR direct-readout data are 1-km resolution, while stored data are 4 km. There are also very high spatial resolution (500 m) Defense Meteorological Satellite Program data available in visible/NIR (0.4-1.1 μm) and LWIR (10-12 μm) bands that are helpful in determining smaller-scale spatial attributes of cirrus.

In the first Scientific Report to this contract, a technique to retrieve cirrus optical properties from multispectral infrared data available from the AVHRR sensor is described. The algorithm requires satellite measurements of the cirrus cloud at two infrared wavelengths, one MWIR and one LWIR. In addition, a theoretical relationship between the cirrus emissivity at both wavelengths must be established. With this information the algorithm uses a series of three equations to compute the effective physical temperature of the cloud (T_{cld}) and its bulk emissivity at each wavelength (ε_{MWIR} and ε_{LWIR}). The equations are as follows:

$$I_{obs,MWIR} = (1 - \varepsilon_{MWIR}) I_{sfc,MWIR} + \varepsilon_{MWIR} I_{cld,MWIR} \qquad (1a)$$

$$I_{obs,LWIR} = (1 - \varepsilon_{LWIR}) I_{sfc,LWIR} + \varepsilon_{LWIR} I_{cld,LWIR} , \qquad (1b)$$

and

$$\varepsilon_{MWIR} = 1 - (1 - \varepsilon_{LWIR})^m .\qquad (1c)$$

where I_{cld} is the cirrus Planck blackbody radiance which is a known function of the cirrus effective temperature (T_{cld}), I_{sfc} is the background (below the cloud) blackbody radiance obtained from nearby, non-cirrus IR values, the subscripts MWIR and LWIR refer to the respective IR channels, and m is the slope of a linear fit to theoretically-derived optical depths computed at each wavelength for a range of cloud thicknesses.

The slope m turns out to be well parameterized by ice crystal size, which in turn is strongly associated with cirrus environmental temperature. Ou et al. (1993) parameterize ice crystal size as

$$L = c_0 + c_1 (T\_cld-273) + c_2 (T\_cld-273)^2 + c_3 (T\_cld-273)^3 \qquad (2)$$

where L is the effective ice crystal size (μm); { c_0, c_1, c_2, c_3 } = { 326.3, 12.42, 0.197, 0.0012 }; and where T_{cld} is the cirrus effective temperature (K). The slope m is then given by:

$$m = a_0 + a_1 / L + a_2 / L^2 , \qquad (3)$$

where { a_0, a_1, a_2 } = { 0.722, 55.08, -174.12 } (after Ou et al., 1993). Figure 1 contains a plot of the regression slope m as a function of cirrus effective temperatures T_{cld} between 210 K and 253 K.

Eqs. (1a), (1b), and (1c) can be used with AVHRR Channels 3 and 4 or 3 and 5; and GOES Imager Channels 2 and 4, or Channels 2 and 5. Thus, for every triplet of AVHRR or GOES infrared satellite radiance measurements ($I_{obs,i}$, $I_{obs,j}$, and $I_{obs,k}$) it is possible to retrieve at sensor resolution the 3.7-3.9 (i), 10.7 (i), and 11.8 μm (k) cirrus bulk emissivities ε_i, ε_j, ε_k and optical depths δ_i, δ_j, δ_k along with cirrus effective temperature (altitude) T_{cld} (z_{cld}).

An inherent assumption in Eqs. (1a) and (1b) is that any reflection from the cirrus cloud can be neglected. At LWIR wavelengths, this assumption is reasonable since both the cirrus bulk reflectivity is low and there is only minor downwelling thermal energy incident on the top of cirrus clouds to be reflected back to space. However, for the MWIR data reflection of incident solar energy during daytime cannot be considered negligible and the validity of Eq. (1a) becomes suspect. If the series of Eq. (1a), (1b), and (1c) do not provide an accurate description of the radiant energy balance then the cirrus retrieval process becomes considerably more complex. Ou et al. (1993) have developed a technique to separate out the solar component in the 3.7 μm daytime data that is potentially applicable to this problem.

Based on this issue, use of Eqs. (1a), (1b), and (1c) should be limited to nighttime scenes when there is no incident solar energy being reflected back to space by either the cirrus cloud itself or the underlying background.
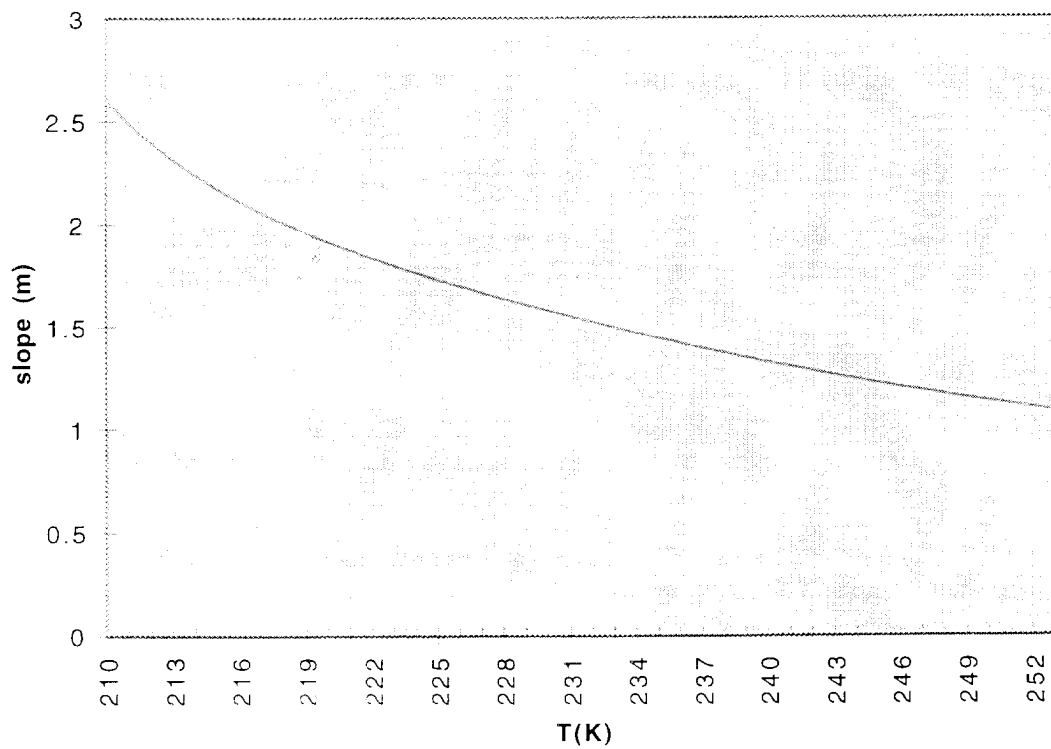
Figure 1.   Plot of "m" in Eq (1c) as a function of cirrus effective temperature T_{cld}.

-4

2.1 CIRRUS RETRIEVALS USING 6.7-μM WATER VAPOR IMAGER DATA

Pursued in light of the 3.7-μm daytime solar contamination issue, ongoing studies are revealing that 6.7-μm water-vapor channel data can be used for the MWIR-channel data in place of those taken at 3.7-3.9 μm data used above in the cirrus retrieval algorithm. This finding is significant in that (a) the complexity of retrieving cirrus properties during daytime (due to mixed solar/thermal energy at 3.7-μm) is eliminated, and (b) there are 6.7-μm water vapor channels on all currently operational meteorological satellites, both geostationary and polar, save DMSP. Thus, with the development of a 6.7-μm cirrus optical depth and effective altitude algorithm comes a capability for cirrus spatial and optical property analyses that are truly global in nature and that span the full diurnal cycle. The water-vapor cirrus retrieval physics is identical to the MWIR retrieval physics in that 6.7 μm-derived radiances are used Eq. (1a) is written for 6.7-μm (vice 3.7-μm) satellite radiance observations, and that Eq. (2) and (3) are replaced by

$$m = 1 , \qquad\qquad (4)$$

the underlying premise being that cirrus optical properties are very similar between 6.7 and 10.7 μm (Kuo-Nan Liou, personal communication).

2.2 CIRRUS RETRIEVAL RESULTS

Comparisons between SERCAA and coincident ground-based observations of cirrus cloud were made over Wisconsin and Hanscom AFB during SBIRS field experiments. Before discussing in detail the comparison results, it is first worthwhile to discuss differences in the data source platforms. SERCAA cirrus cloud top and optical depth analyses are provided at meteorological satellite sensor resolution, which is 1 km for AVHRR and 4 km for GOES-Next. CO_2 Slicing analyses for HIRS data are nominal 17 km, and for GOES-8 are 8 km. In stark contrast, coincident ground-based lidar and radar observations have spatial resolutions on the order of meters. In addition, there are obviously significant differences between satellite imagers and ground-based radars/lidars in spectral bandwidths and band locations. Thus, some platforms such as the lidars will be much more sensitive to tenuous, very thin cirrus than will be a passive infrared meteorological satellite radiometer. There are also time discrepancies and geo-location errors inherent in the multiple ground- and space-based data sources, although every effort was expended to insure these were kept to an absolute minimum.

With all these factors in mind, the question arises of what is reasonable to expect for "agreement" when comparing such diverse analyses and observations. Although the SERCAA and lidar/radar comparisons are as quantitative as possible, they cannot be performed in an absolute sense. In this light, comparisons were evaluated with one major theme in mind, namely, whether the observations dispute the satellite-based retrievals.

Initial retrieval results over a 10-case data set do not conflict with ground- and aircraft-based observations of cirrus clouds. Figures 2-10 compare directly the SERCAA satellite-based cirrus retrievals with coincident ground-based TPQ-11 35-GHz radar observations of cirrus base and top. The ground-based radar data were collected as a part of the Space-Based Infrared Systems (SBIRS) field experiments conducted over Hanscom AFB, MA and Madison, WI during mid-September 1995. First, three examples are shown

5

of cirrus altitude retrievals plotted against radar altitude observations for 2330 UTC at Hanscom AFB on 16 September 1995.

The colors in Figure 2 are representative of the reflected power received as a function of altitude by the active 35-GHz radar, with warm colors (reds, oranges, yellows) corresponding to strong returns and cool colors (green, cyan) corresponding to weaker returns. Dark blue denotes cloud-free observations. Red diamonds denote the SERCAA GOES-8 Imager 3.7-10.7-μm satellite-retrieved cirrus altitudes that correspond with their respective coincident radar observations. As can be seen, the retrievals match well with observation. Corresponding cirrus effective emissivities are plotted in green squares against the right-hand vertical (emissivity) axis. It is seen that the retrieved emissivities are higher where the radar.returns are stronger and vice versa.

Figure 3 is similar to the first, except that it contains results obtained using GOES-8 6.7-μm water vapor image data in place of the MWIR. Yellow diamonds denote the SERCAA 6.7-10.7-μm satellite-retrieved cirrus altitudes that correspond with their respective coincident radar observations. The 3.7-μm retrievals (Figure 2) and the 6.7-μm retrievals (Figure 3) are coincident in time and space, and are both from the GOES-8 Imager. The water-vapor retrievals also match well with observation. However, the water-vapor altitude retrievals agree more closely to the true tops of the transmissive cirrus, in comparison to the respective 3.7-μm MWIR retrievals. The closer agreement is due primarily to the fact that in the cirrus environment there is more atmospheric water vapor than in the "clear-column" (i.e., cirrus-free) regions. The net result is that the 6.7-μm cirrus brightness temperature observations are more strongly influenced by this excess water vapor than are the corresponding 3.7-μm MWIR measurements, since the 3.7-μm spectral region is an atmospheric window wherein water-vapor absorption effects are minimal. There are two useful attributes to this deterministically explainable "bias." The first is that for the SBIRS program, cirrus cloud top altitudes are generally of more value than the "radiative center-of-mass" altitudes that the 3.7-μm data provide. The second is that in differencing the MWIR and water-vapor altitude retrievals, information on cirrus physical thickness can be inferred that has to now been unobtainable using passive infrared retrieval techniques.

Figure 4 is a simple plot of AVHRR-retrieved 3.7-μm cirrus effective altitudes with the corresponding 35-GHz radar observations. The radar-observed cirrus tops and bases are plotted as brown and cyan lines, respectively. The blue diamonds denote the 1-km pixel-by-pixel NOAA AVHRR cirrus altitude retrievals; they compare well with observation, as did their GOES Imager counterparts. The green squares correspond to "blackbody" altitude retrievals obtained using 10.7-μm brightness temperatures that have been uncorrected for cirrus transmissive effects, i.e., assuming cirrus is a blackbody cloud. This is the technique used by many cloud analysis models that compute cloud altitude for both opaque and transmissive clouds. Altitudes retrieved in this manner agree reasonably well with true cirrus altitudes wherever cirrus transmissivities are low (optically thick cirrus), as is seen on the left side of the plot. However, where cirrus is optically thin, the comparison differences are dramatic: on the right half of the plot are cirrus blackbody retrievals that differ by as much as 6 km from the true, SERCAA-retrieved cirrus altitudes. It is important to note that the green squares denote state of the art in the current Air Force operational global cloud analysis model, the RTNEPH, as well as in the Phase-I SERCAA algorithms being implemented as a part of CDFS-II.

Figures 5-7 contain plots of SERCAA cirrus effective altitudes and emissivities for NOAA 3.7, GOES-8 3.7, and GOES-8 6.7-μm/10.7-μm retrievals, respectively, over Hanscom AFB earlier on the afternoon of 16 September 1995. The NOAA overpass time
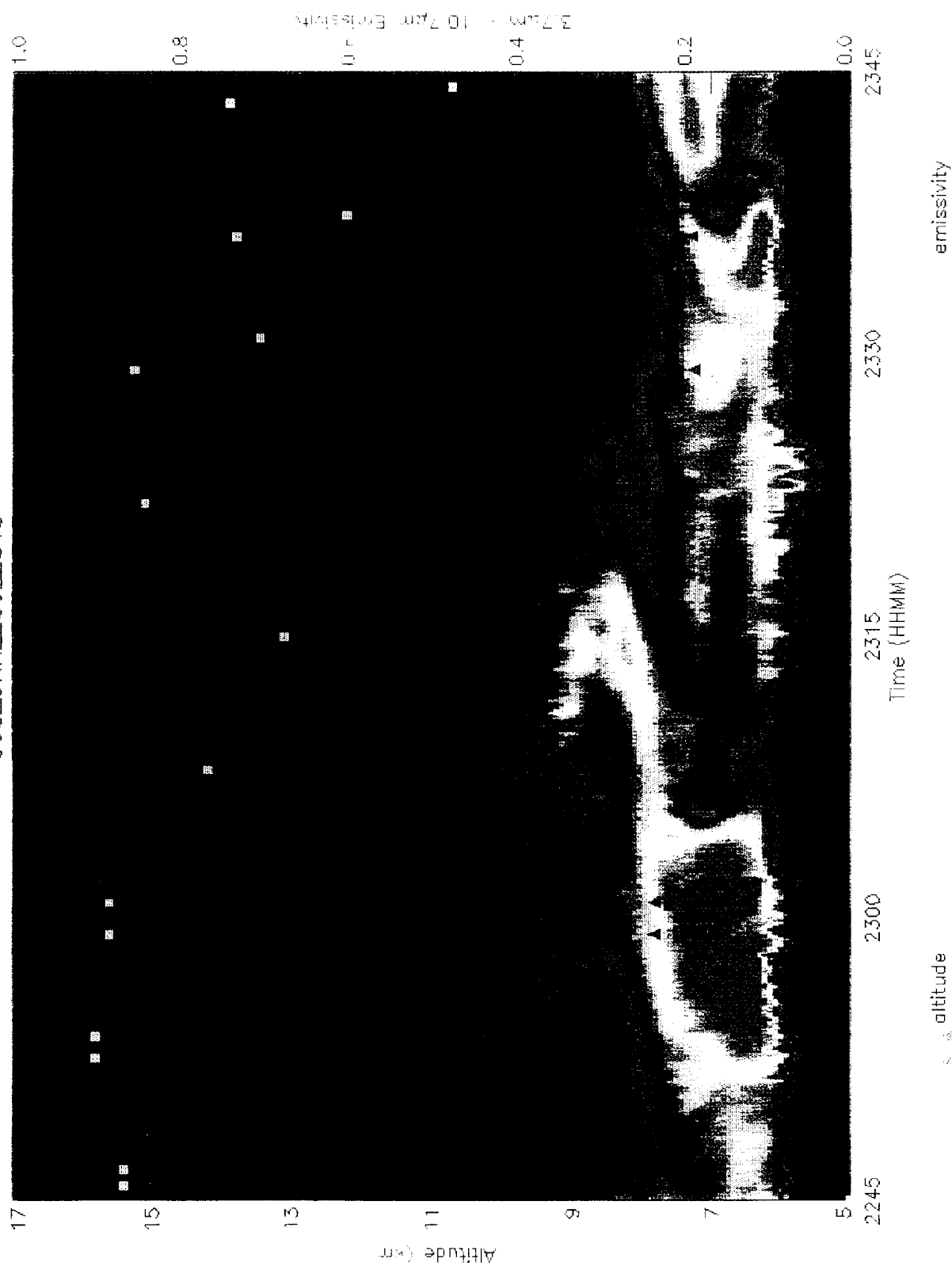
Figure 2. SERCAA GOES-8 MWIR cirrus altitude and emissivity retrievals over Hanscom AFB at 2315 UTC on 16 Sep 95, plotted with corresponding surface-based-radar cirrus observations.
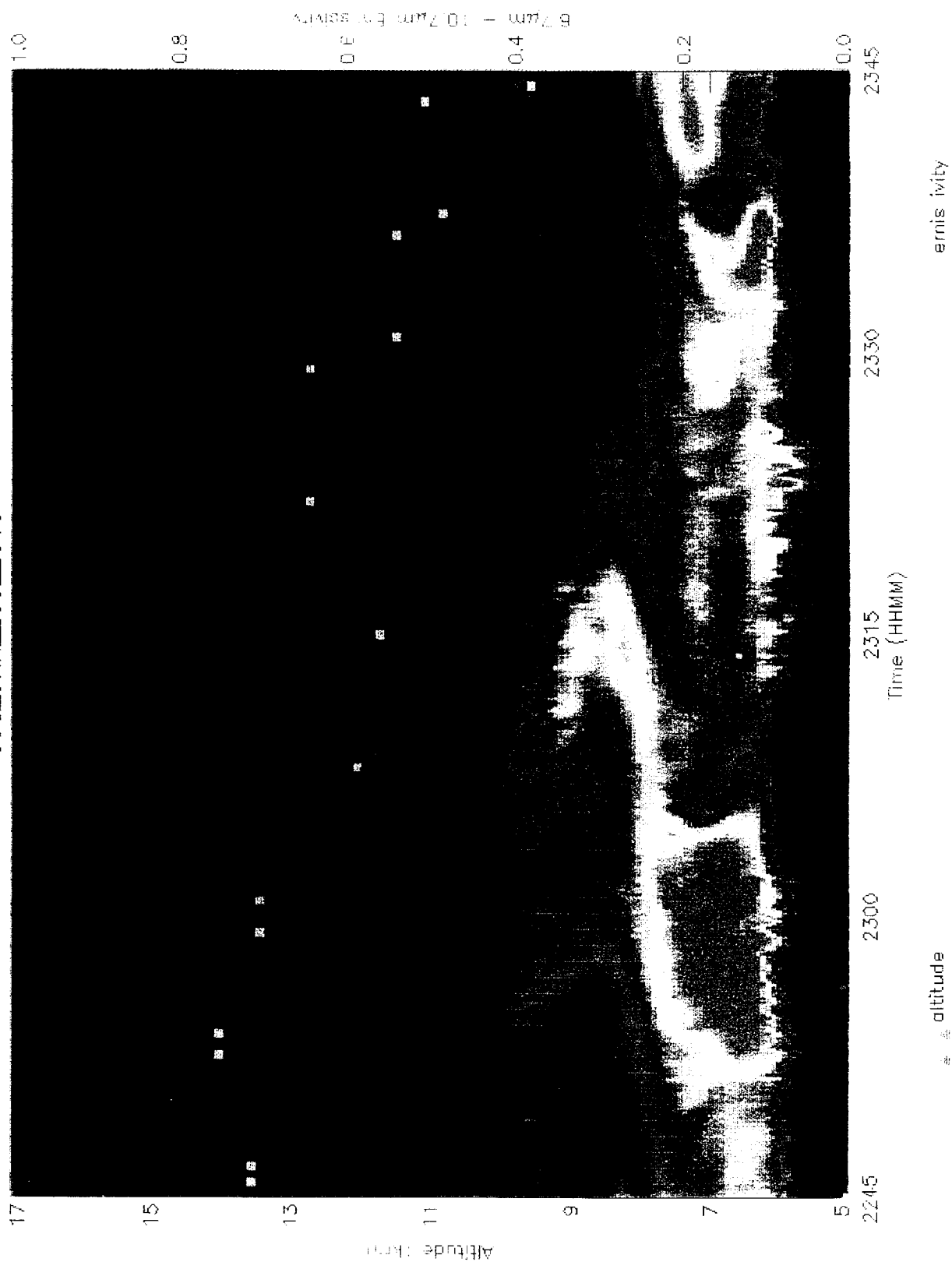
Figure 3. SERCAA GOES-8 water-vapor cirrus altitude and emissivity retrievals over Hanscom AFB at 2315 UTC on 16 Sep 95, plotted with corresponding surface-based-radar cirrus observations.
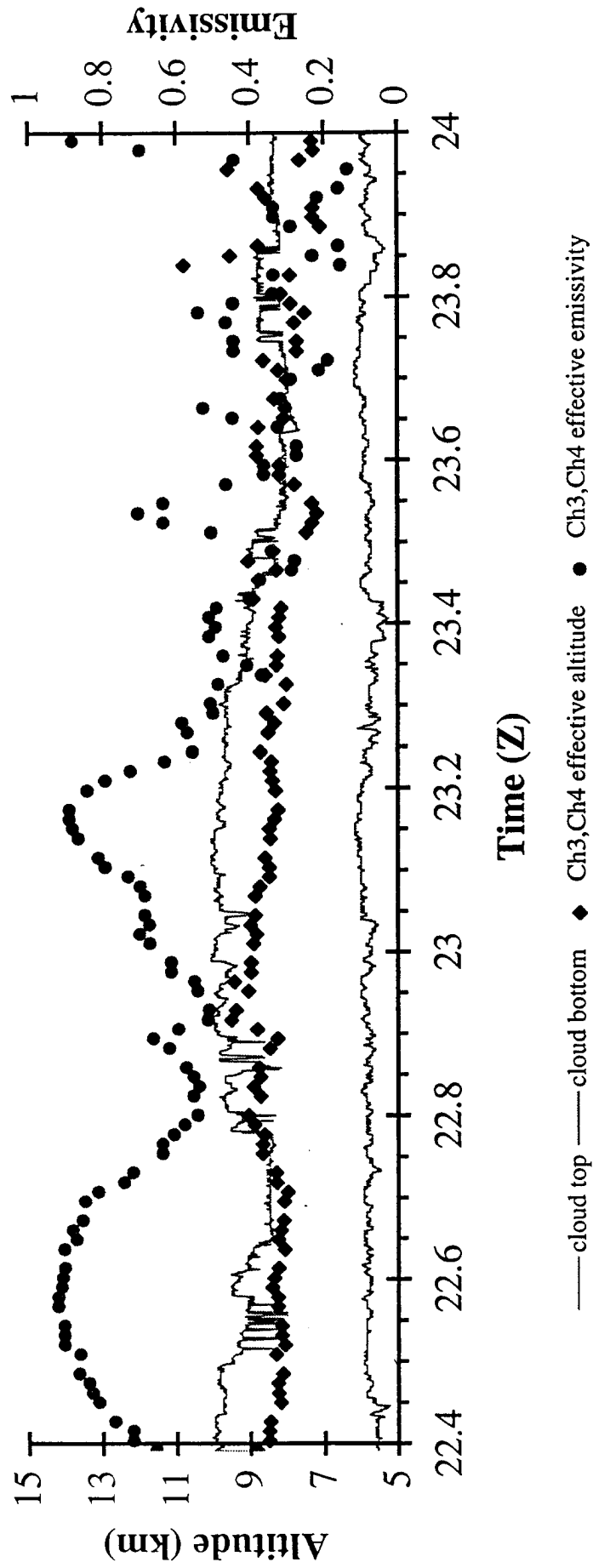
Figure 4. SERCAA AVHRR MWIR cirrus altitude and emissivity retrievals over Hanscom AFB at 2330 UTC on 16 Sep 95, plotted with corresponding surface-based-radar cirrus observations.

9
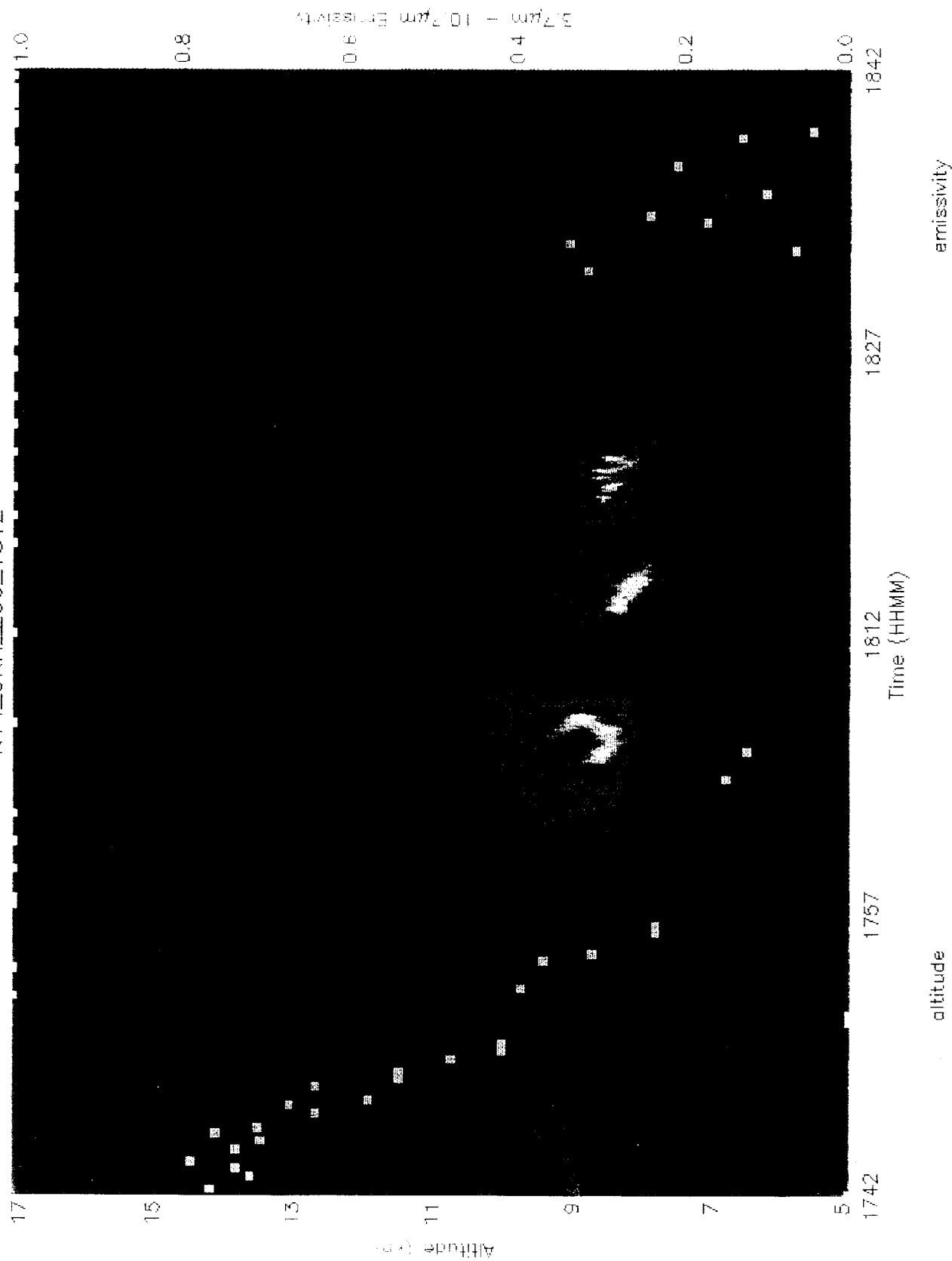
Figure 5.   SERCAA AVHRR MWIR altitude and emissivity retrievals and corresponding radar observations over Hanscom AFB at 1812 on 16 Sep 95.
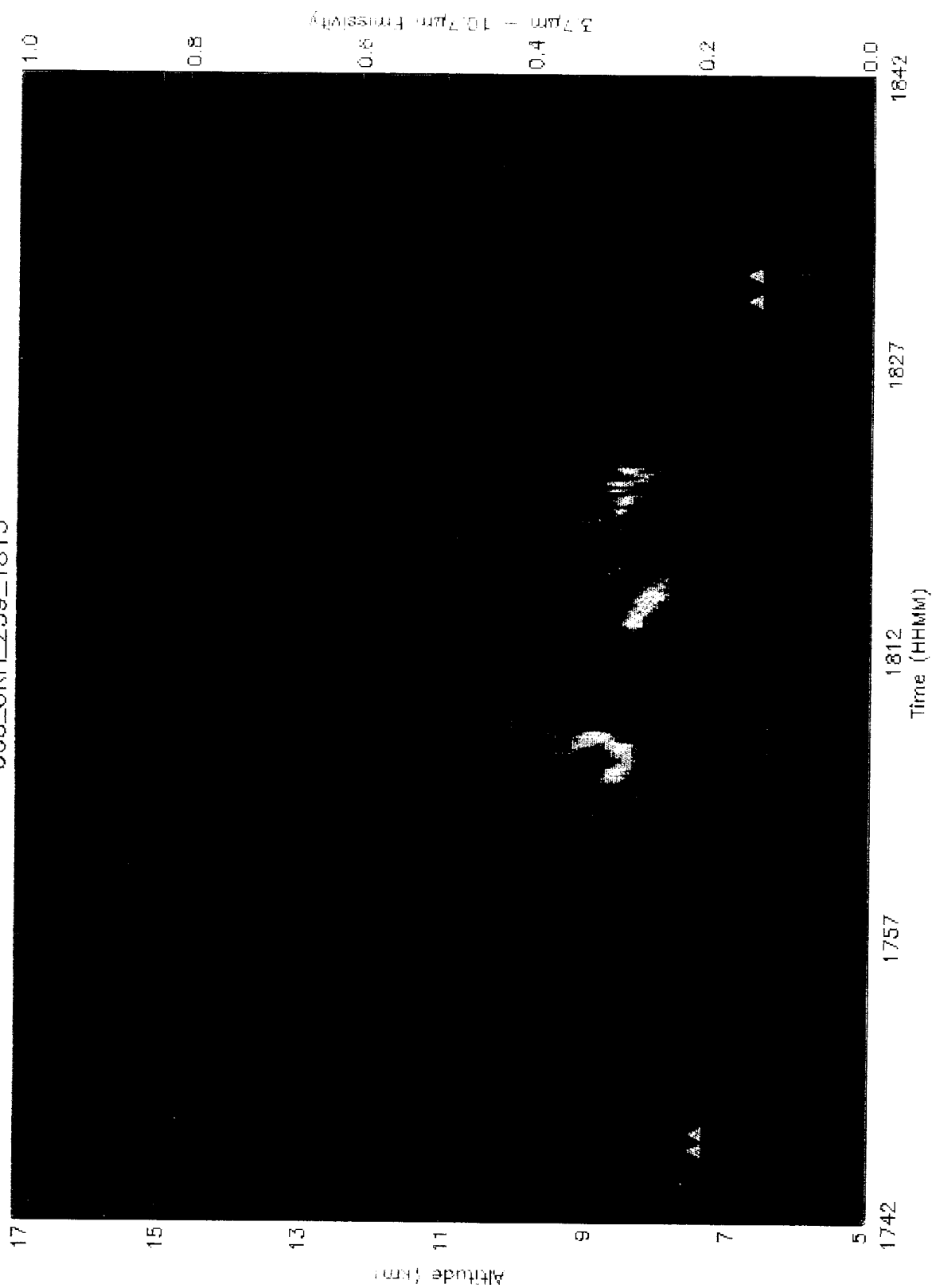
Figure 6. SERCAA GOES-8 MWIR altitude and emissivity retrievals and corresponding radar observations over Hanscom AFB at 1815 on 16 Sep 95.
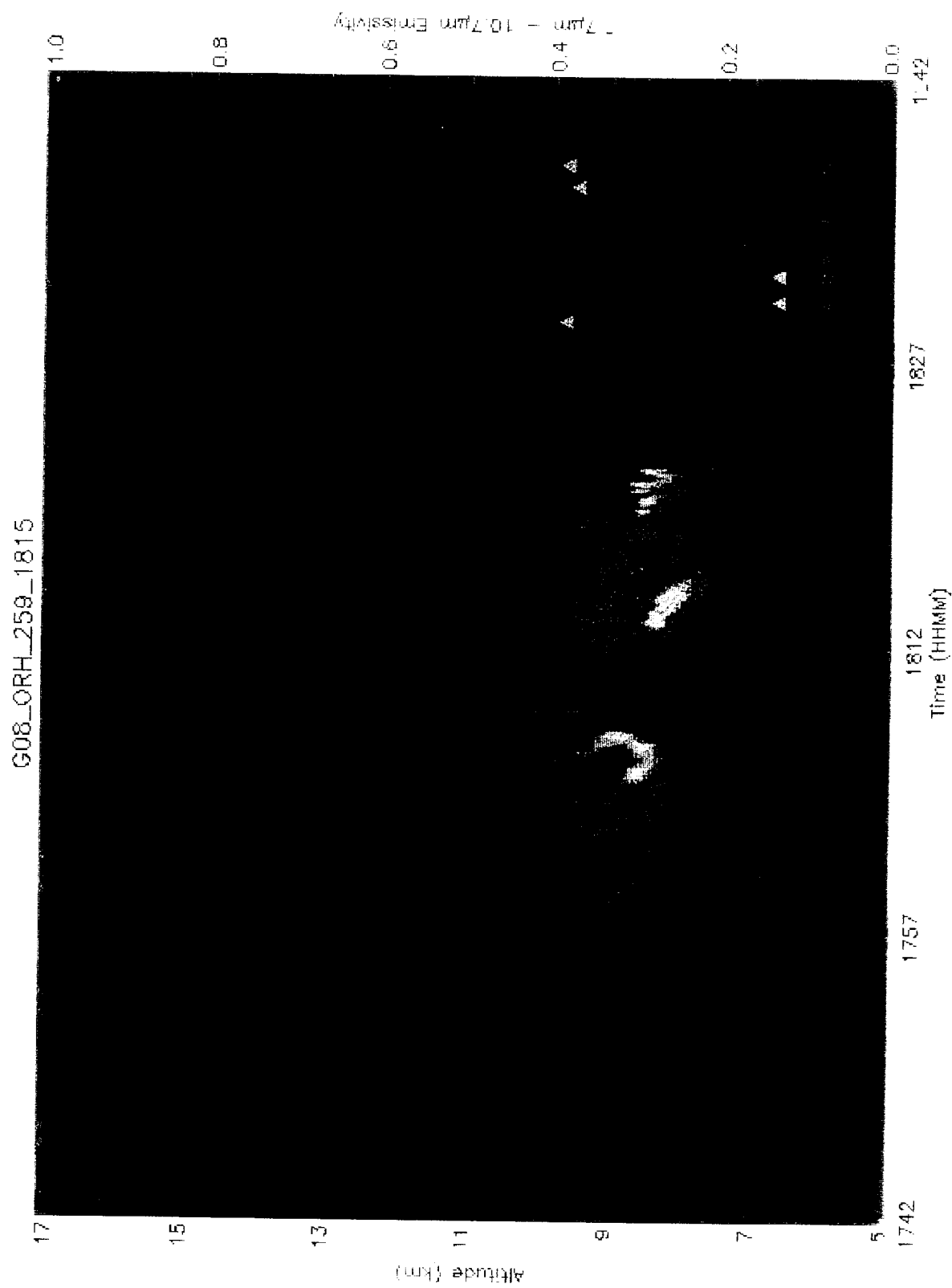
Figure 7.   SERCAA GOES-8 water-vapor altitude and emissivity retrievals and corresponding radar observations over Hanscom AFB at 1815 on 16 Sep 95.

was 1812 UTC, and the GOES-8 Imager time was 1815 UTC. Again, the bulk of the retrieved altitudes are not in dispute with the TPQ-11 radar observations. Finally, Figures 8-10 contain plots of SERCAA retrieval results for 1815 UTC on 25 September 1996 over Hanscom AFB for NOAA AVHRR (Figure 8) and GOES-8 Imager (Figures 9, 10) data. Note that the GOES water-vapor cirrus altitude retrievals are up to 1 km higher than the 3.7-μm retrievals, as noted previously.

Similar comparisons were made between SERCAA altitude retrievals and the University of Wisconsin (UW) High Spectral Resolution Lidar (HSRL) near Madison WI at 1915 UTC 4 August and 2315 UTC 7 September 1995. On 4 August HSRL backscatter cross section (BCS) observations showed cirrus between 10 and 12 km. NOAA-14 AVHRR retrievals of the same cloud system fell within the same 10-12 km range, with the average cloud altitude at 11 km. As mentioned in Section 2.1, the 11-km average altitude is more representative of the radiative center of mass of the cirrus clouds, and not their true tops. GOES-8 3.7-μm retrievals for the same time fell in the 9-11 km range, with an average altitude of 10 km, all in all slightly lower than the AVHRR retrievals. The GOES 6.7-μm water-vapor retrievals show altitudes between 9 and 12 km, with an average altitude of 11 km. Note again that the SERCAA water-vapor average altitude is 1 km higher than that obtained using the 3.7-μm data.

On 7 September HSRL BCS observations indicated cirrus between 8 and 12 km. GOES-8 3.7-μm retrievals for the same time fell in the 9-10 km range, with an average altitude of 9.5 km. The GOES 6.7-μm water-vapor retrievals show altitudes between 10 and 11 km, with an average altitude of 10.5 km. Yet again, the SERCAA water-vapor average altitude is 1 km higher than that obtained using the 3.7-μm data.

UW Volume Imaging Lidar (VIL) observations were also compared to SERCAA cirrus altitude retrievals. Figure 11 shows VIL BCS cloud-top observations between 8 and 11 km near Madison at 2234 UTC on 14 September 1995. SERCAA altitude retrievals using coincident GOES-8 3.9/10.7-μm data range between 7.3 and 8.9 km. Water vapor data failed to detect the thin cirrus. Figure 12 shows 2038 UTC 26 September 1995 VIL BCS cirrus cloud top observations between 7 and 10 km. SERCAA altitude retrievals using coincident GOES-8 3.9/10.7-μm data range between 3.9 and 8.6 km. However, this time the water vapor data detected the thin cirrus and the corresponding SERCAA altitude retrievals fell between 9.6 and 10.2 km. Again in large part the SERCAA cirrus effective altitude retrievals are not in dispute with the VIL observations.

Finally, subjective comparisons between CO_2 Slicing and SERCAA cirrus altitude retrievals were made for several AVHRR overpasses during the SBIRS September 1995 observation period. An example is shown in Figure 13, which contains a pseudo-image of the 1-km-resolution SERCAA cirrus altitudes for 2335 UTC 16 September over New England. Plotted over the image in black squares are the coincident CO_2 Slicing altitudes. Except for the CO_2 Slicing cloud top in the extreme upper right of the image, agreement between the two independent analyses is strong. Comparisons over Wisconsin bore similar results.

2.3 SUMMARY

As a part of SERCAA cloud analysis development efforts, new and innovative multispectral infrared cirrus analysis techniques have been developed, successfully applied, and compared to SBIRS cirrus detection, analysis, and ground-based observation
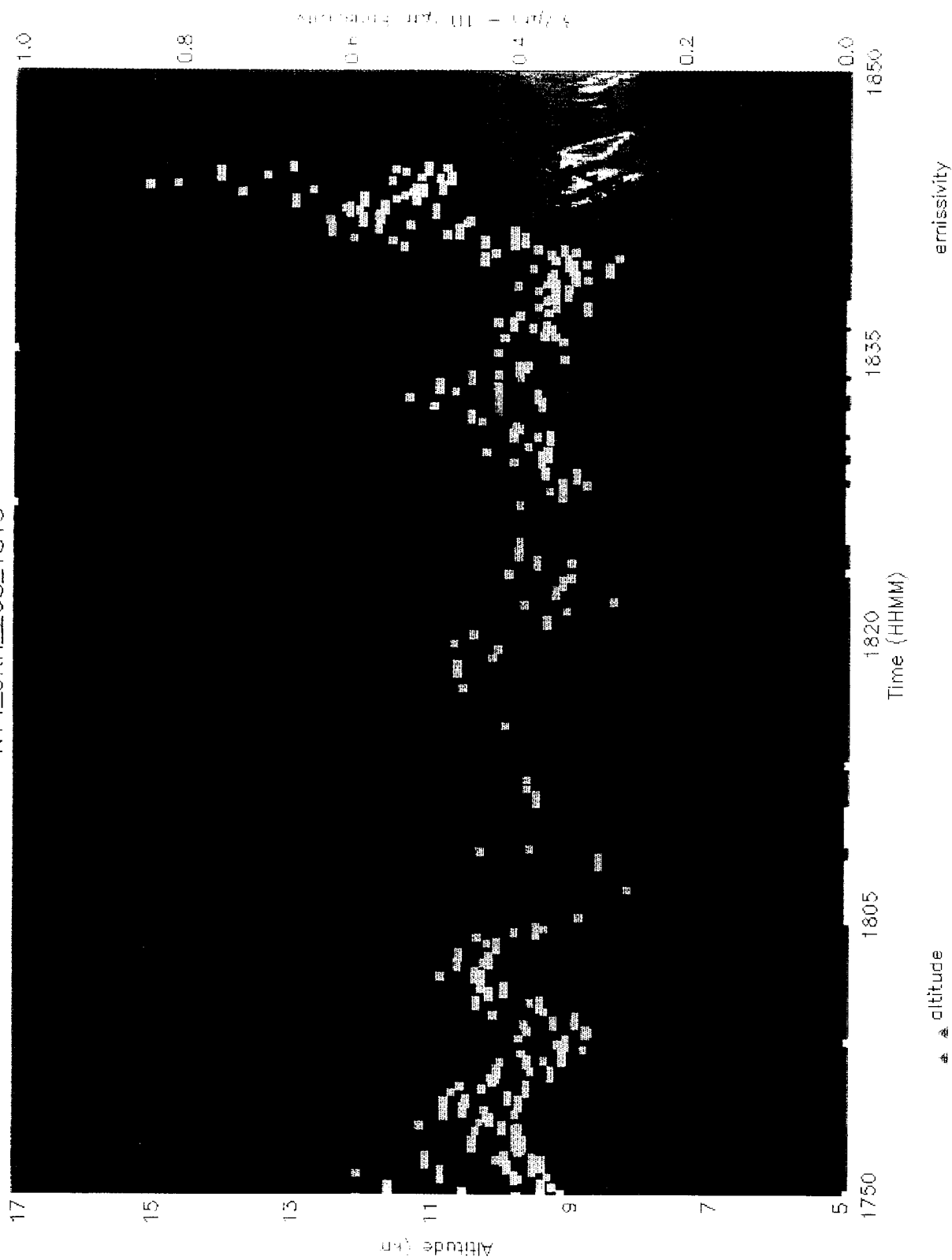
Figure 8.   SERCAA AVHRR MWIR altitude and emissivity retrievals and corresponding radar observations over Hanscom AFB at 1815 on 25 Sep 95.
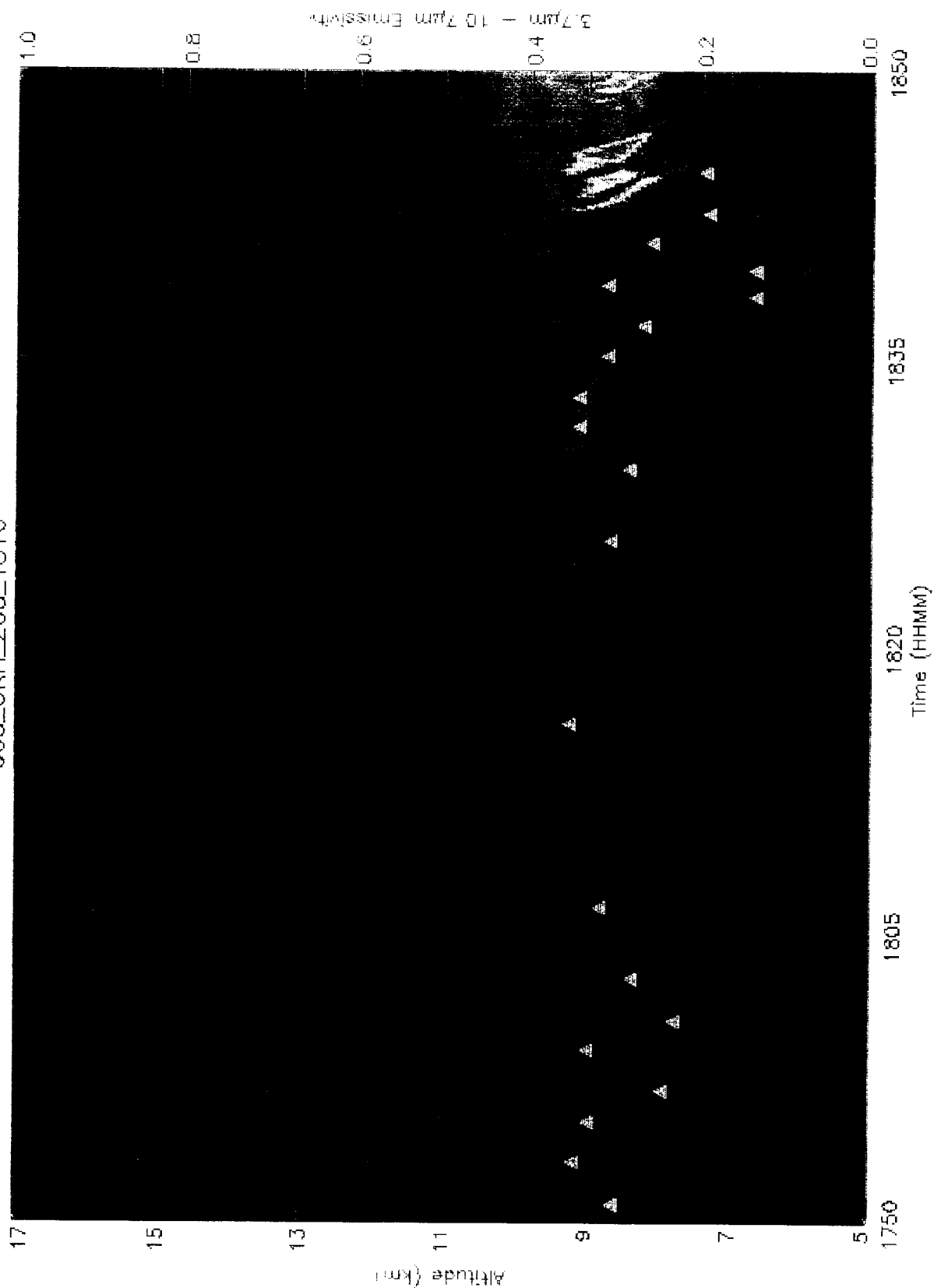
Figure 9. SERCAA GOES-8 MWIR altitude and emissivity retrievals and corresponding radar observations over Hanscom AFB at 1816 on 25 Sep 95.
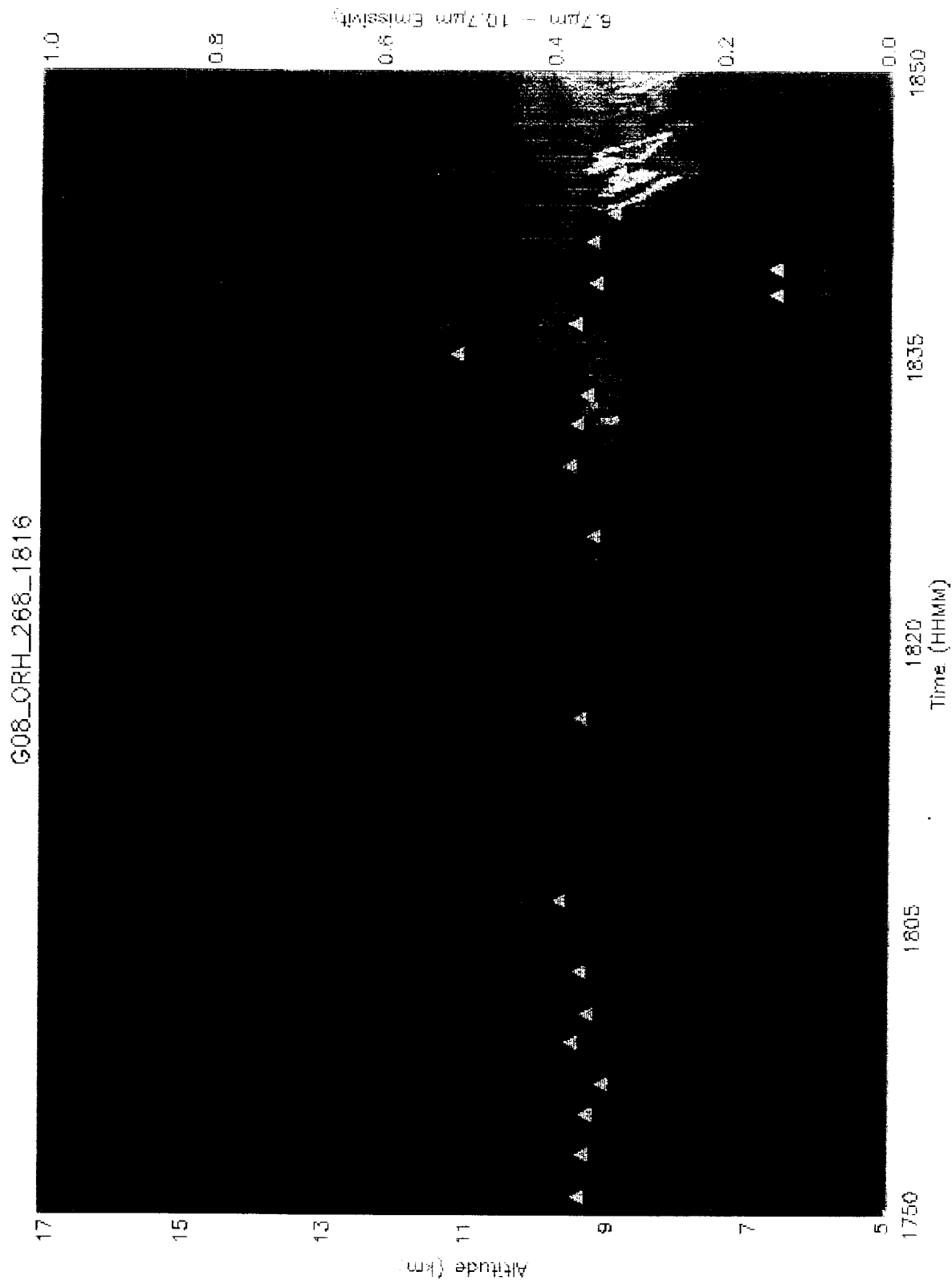
Figure 10.   SERCAA GOES-8 water-vapor altitude and emissivity retrievals and corresponding radar observations over Hanscom AFB at 1816 on 25 Sep 95.

University of Wisconsin–Madison Lidar
VIL Cloud Top BCS=1e-6
14-September-1995 22:34:30 UT

11000   10500   10000   9500
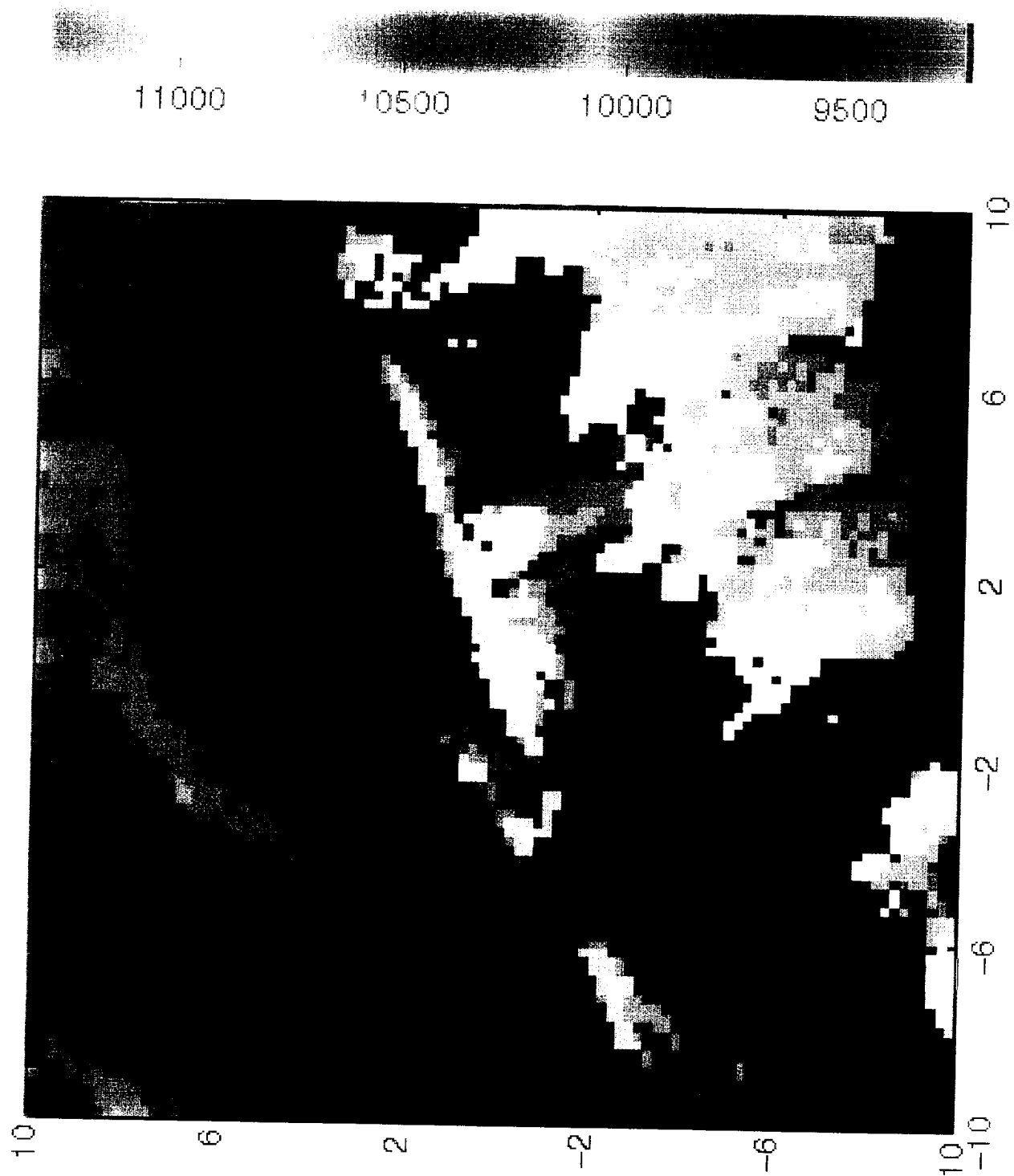
Figure 11. University of Wisconsin VIL cirrus back scatter cross section observations near Madison at 2234 UTC on 14 Sep 95.

University of Wisconsin–Madison Lidar
VIL Cloud Top BCS=1e-6
26-September-1995 20:38:00 UT
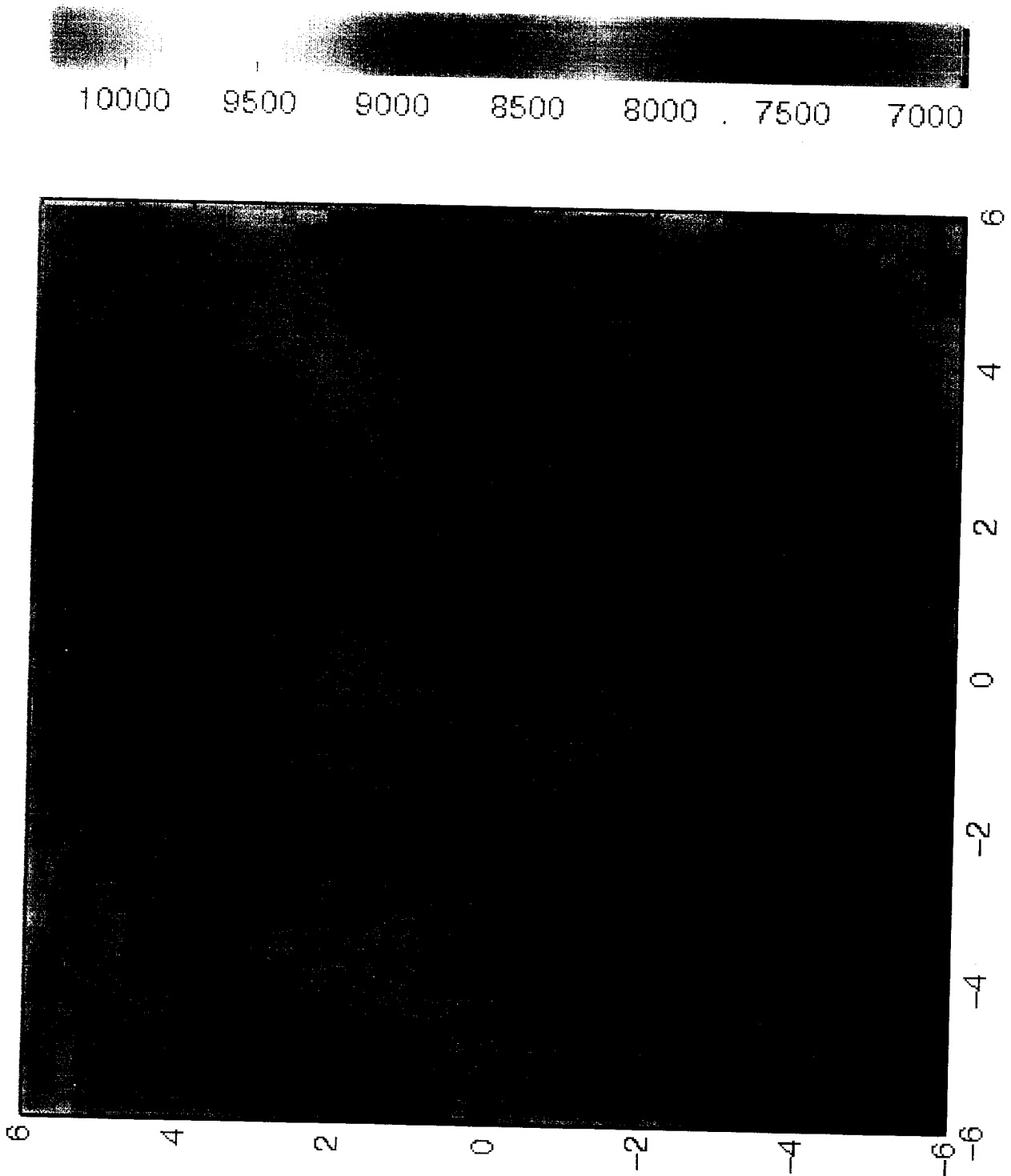
Figure 12. University of Wisconsin VIL cirrus back scatter cross section observations near Madison at 2038 UTC on 26 Sep 95.
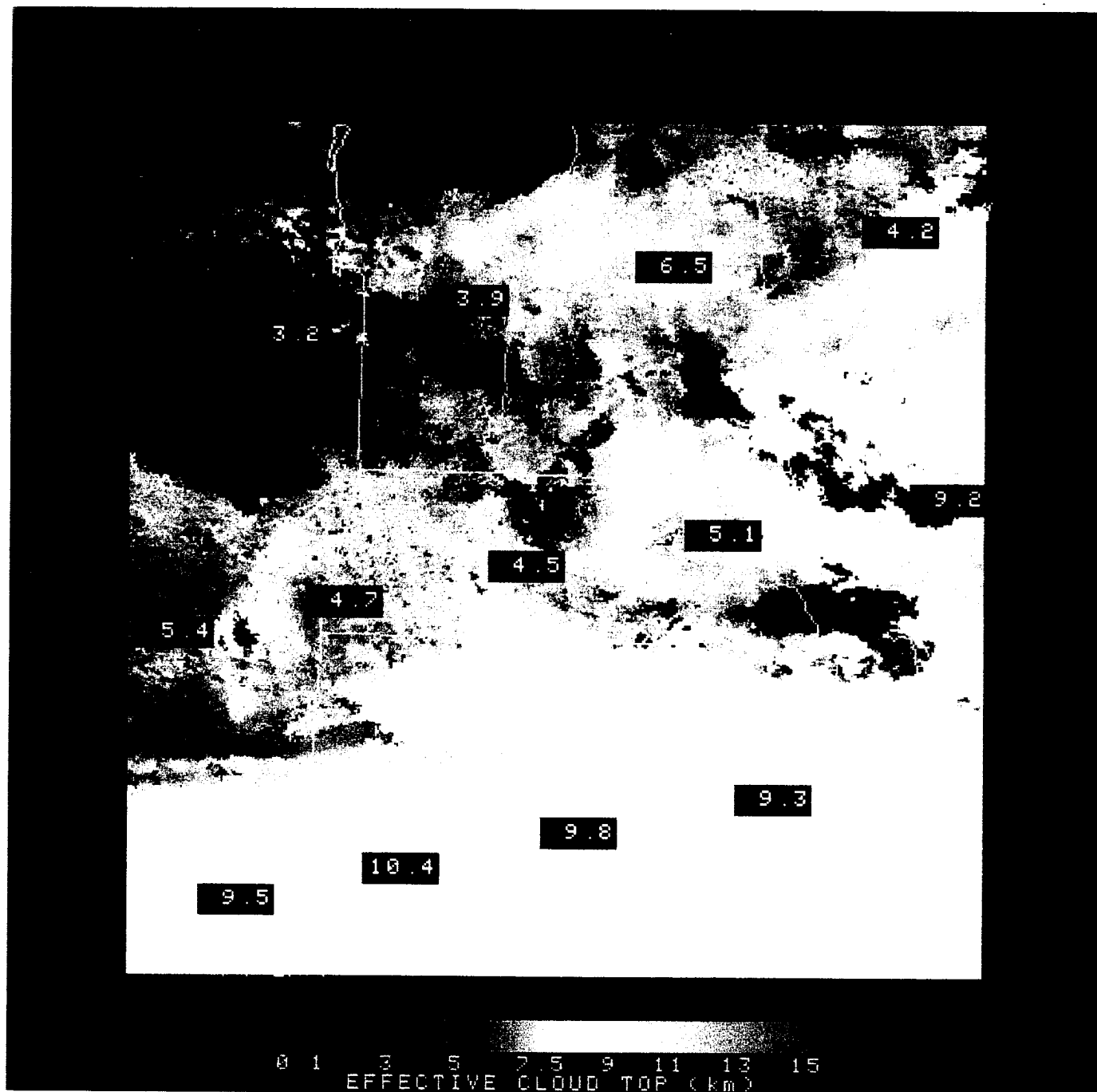
Figure 13. SERCAA cloud effective altitude retrievals using NOAA AVHRR MWIR data over New England at 2330 UTC on 16 Sep 95. Plotted over the analysis in black squares are the coincident CO_2 Slicing altitude retrievals. Spatial resolution of the SERCAA analysis is nominal 1 km; CO_2 Slicing analysis resolution is nominal 17 km.

scenarios. Integration of these and other retrieval techniques into the overall SERCAA cloud analysis allows the strongest and most reliable attributes of each technique to be combined into one comprehensive cloud analysis product that is more realistically representative of cirrus spatial and optical properties than the current RTNEPH. With increasing amounts of multispectral infrared satellite data becoming available, the goal is to continue to retrieve from these data high quality augmented radiative, spatial, and microphysical properties of cirrus clouds in real-time and for climatological purposes at finer spatial and temporal resolution.

3. SBIRS ANALYZED DATA SETS

The SBIRS Phenomenology Exploitation Project (PEP) is investigating the impact of cloud on proposed systems. In support of that project, two months of high resolution AVHRR and GOES data were analyzed to retrieve cloud distribution information over the central and eastern U.S. and the western Atlantic (Figure 14). The AIMS NOAA and GOES satellite ground stations were used to acquire all AVHRR data over the region of interest from NOAA 12 and 14 and three-hourly GOES-8 data (0,3,6,9,12,15,18,21 Z) during the months of August and September 1995. Occasional time periods are missing due to GOES eclipse periods and missing/bad data. Basic cloud-detection processing was performed using the SERCAA Phase 1 and 2 algorithms described by Gustafson et al. (1994). Further processing then occurred using the cloud phase and cirrus altitude retrieval algorithms described in Section 2 above. The final products are pixel-level representations of cloud amount as a function of optical-property-retrieval-corrected altitude, pressure, and emissivity. Additional data includes latitude and longitude for each pixel. Appendix A contains a description of the output data products and the format of the data as provided to the PEP.

3.1 DATA PROCESSING

The SBIRS Optical Property retrieval program (SOP) described in Section 2 was used to assign cloud-top altitude, emissivity and pressure for each scene. Processing was performed on a per pixel basis using a cloud mask generated by the SERCAA cloud analysis program. The same program was used on both the NOAA and GOES data. Results are presented as a series of 8-bit TIFF files, each at the same resolution as the input satellite data. Altitude, pressure, emissivity at 3.7, 6.7, and 10.5 μm and geo-location data were produced. Retrievals were evaluated for meteorological validity and spatial uniformity. Approximately 100 images were inspected to assure consistency of results.

SOP consists of five modules: satellite data ingest, clear column temperature calculations, upper air retrieval, an implementation of the cirrus emissivity/altitude algorithm and product generation.

Satellite Data Ingest: Satellite data required for the cirrus emissivity/altitude algorithm are 3.9, 10.5 and 11.5 μm channel imagery from AVHRR and 6.7, 10.5, and 11.5 μm data from GOES. All sensor data were archived using the AIMS SERCAA Database (SDB). In SDB, images from a satellite pass are stored as scaled 8-bit pixels at a fixed resolution for each satellite system, for AVHRR this is 1 km, for GOES it is 4 km. The data ingest module calibrates and Earth locates the satellite telemetry data and produces the database records.
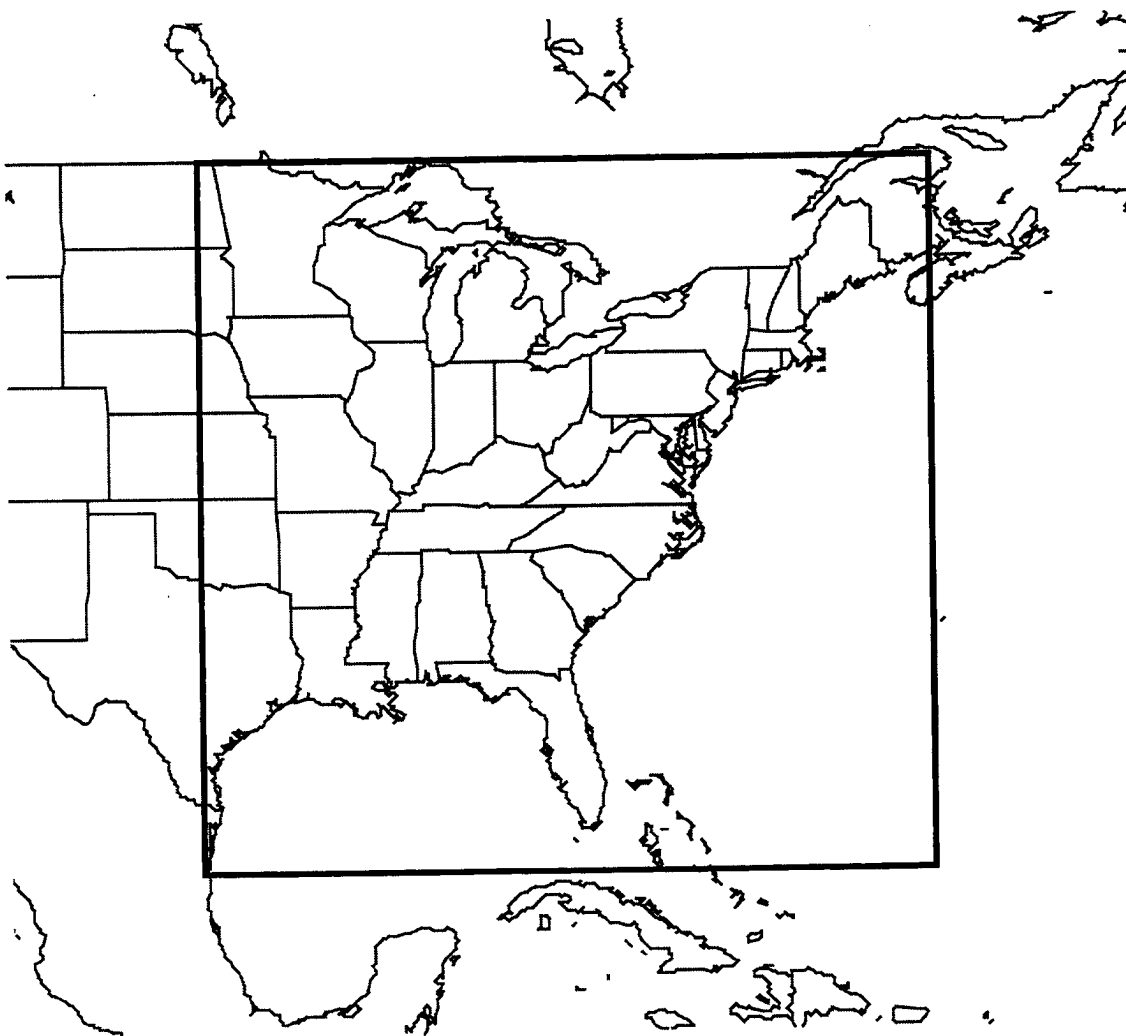
Figure 14. Region of data collection and analysis for the SBIRS PEP.

Clear Column Temperature Calculation: cloud property retrievals are based on the deviation of the observed temperatures from reference clear column temperatures, therefore the calculations are highly sensitive to both the absolute value and the variation of clear column temperature within a scene. Competing requirements of accuracy in retrieved properties and "smoothness" of expected results led us to evaluate a variety of strategies for determining clear column temperatures.

Climatology data derived from the AFGWC SFCTMP program were evaluated as a source for clear column temperatures. This provided smooth results at the expense of accuracy. A conscious goal was to minimize reliance on climatology and utilize contemporaneous satellite imagery data.

Initially we assumed that the nearest cloud-free (CLEAR) pixels would provide the most accurate surface temperature estimate. For each cloudy pixel, we searched the scene to find the n closest pixels identified as CLEAR in the cloud mask, where n was allowed to vary from 3-50 pixels. The resulting altitude assignment was "blocky" (piecewise continuous) and a function of the search distance required to locate the CLEAR pixels. We constrained the search to 200 km radius and imposed a low limit (7) on the number of pixels averaged. Climatology was used for pixels where no nearby clear data could be found. This improved the results, although discontinuities were still observed and run times were excessively long (e.g., >100 min. for 500 x 1500 pixels).

With such large search neighborhoods, we decided that accuracy would not be sacrificed if we used the same clear column temperatures for all pixels within a neighborhood. Separate values for geography types (land/water) were maintained since combined types removed natural variation and distorted the altitude results. Clear-scene temperature calculations occur only twice per neighborhood, once each for land and water backgrounds. Processing performance improved by more than an order of magnitude with no noticeable loss of accuracy.

For large cloud masses, discontinuities in retrieved cloud altitude were introduced when the clear scene temperatures were chosen from different sides of a cloud mass. This is demonstrated in Figure 15. These artificial discontinuities were removed by providing for overlap of the neighborhoods. Our results showed that substantial overlap on large neighborhoods represented the best approach. In each neighborhood, clear scene temperatures were taken as the average temperature, after eliminating the coldest 5% and warmest 10% of pixels. Separate temperatures were stored for land and water points. Coastal boundary locations were treated as land.

The final processing algorithm works by first dividing the scene into neighborhoods of approximately 700 km^2 for calculation of clear scene temperatures. Results showed that a substantial overlap of approximately 40% of these large neighborhoods produced the most consistent analysis. Figure 16 shows the same image as Figure 15, this time with smoothed, corrected results.

Upper Air Data: Upper air temperature and moisture profiles were used by SOP to convert cloud-top temperature information to cloud altitude and pressure. Gridded LFM analysis fields obtained from NCAR/UCAR for August and September, 1995 were used to provide the required upper air data between 20-50N and 50-100W. Available LFM fields were geopotential height (up to 500 mb), temperature for all available levels (up to 200 mb), dewpoint temperature (up to 300 mb) and surface temperature.

22

Figure 15. Image of cloud-altitude product showing discontinuity in the analysis across the cloud mass in the center of the image.

xv 3.10a: data/good2809.alt <unregistered>

Figure 16. Same analysis as Figure 15 using neighborhood overlap to eliminate discontinuity in the altitude analysis.

24

Twice-daily radiosonde observations were used to augment the LFM fields at upper levels. A latitudinal climatology of temperature, dew point temperature and height was calculated for mandatory pressure levels between 1000 and 200 mb using radiosondes located within the eastern U.S. and Canada. To be used, the sounding had to go up to at least 500 mb and reported pressure interval below 500 mb must be less than 150 mb.

LFM and radiosonde-derived data were combined so that each LFM grid cell contains geopotential height, air temperature, and dew point temperature for 15 levels (i.e., 1000, 950, 900, 850, 800, 750, 700, 650, 600, 550, 500, 450, 400, 300, 250, 200 mb). Radiosonde data were interpolated to the intermediate levels. Any biases between the LFM data and radiosonde data were removed from the radiosonde data at the interface level to produce a smooth continuous profile. The resulting profiles were analyzed for discontinuities and none were found.

Cirrus Emissivity/Altitude: The cirrus emissivity and altitude retrieval algorithms described above in Section 2 were implemented on AIMS and used to analyze the AVHRR and GOES data collected during the two-month period. Sensor data were first analyzed through the SERCAA cloud detection algorithms to discriminate clear and cloudy pixels. Cloud pixels were further segregated into two categories: transmissive cirrus and all others.

Product Generation: Products were generated on a per pixel basis. Images for altitude, pressure and emissivity are 256 grey shade, 8-bit LZW compressed TIFF files. They are viewable using a variety of public domain viewers that support TIFF format (e.g., xv, Khoros, IPW) as well as internally developed satellite image viewers available on AIMS. For each analyzed scene there is a TIFF file for retrieved location, altitude, pressure, and emissivity at 3.7 or 6.7 and 10.5 μm. The data are in the original satellite projection and resolution. Latitude and longitude are stored as C language short integer, using the positive North, East convention. Values given are degrees*100 (e.g., 2935 = 29.35°). Altitude values are scaled in increments of 1/17 km (i.e., 0-255 is Linear 0-15 km). Pressure values are mb*10 (e.g., 63 = 630 mb). Emissivity values are ε*100 (e.g., 21 = .21). Altitude values 1 and 254 are reserved for missing data.

3.2 RESULTS AND LIMITATIONS

The results of SOP were validated manually by visualizing synthetic images of the product fields and through comparisons to ground-based lidar and radar measurements. Two problems remain and cause some altitude fields to contain a few anomalous values (manifested as speckles in a synthetic image). We were able to identify two sets of conditions external to the algorithms which led to these anomalous values.

In one set of cases, pixels on the edges of cloud masses were assigned unreasonably high altitudes. Examination of the data indicated that the measured MWIR temperatures were higher than those for nearby low clouds which were flagged as non-cirrus. A correction factor was developed and applied in these cases. After establishing the clear scene information, a maximum MWIR brightness temperature (after discarding the top 5%) for cloudy, non-cirrus pixels was calculated. This temperature is used to correct height assignments. Experiments showed that for cirrus pixels with a MWIR temperature higher than this maximum, the best approach to calculating optical properties was to treat them as low clouds.

25

The second set of problem conditions are a consequence of the pixel by pixel cloud property retrieval approach. Anomalies due to the variable cloud signatures can occur at cloud mass edges, the intersections of cloud masses of varying altitude, and near the day/night terminator. A correction was applied based on a moving 7x7 pixel frame centered on the pixel being analyzed. If a cirrus pixel is identified as being on an edge, i.e. clear and cirrus both found in the frame, then for retrieval purposes the pixel is treated as non-cirrus. Another correction applied was a check to see if the 3.7-μm brightness temperature of the pixel is within 6.5 K of the clear-column brightness temperature. If it is, the 10.7 μm emissivity is adjusted to be two-thirds of the way between the retrieved emissivity and 1.0. Due to problems discriminating cirrus cloud near the day-night boundary, terminator conditions resulted in far less consistent retrievals. Any pixels for which there was an anomalously high retrieved cloud altitude (> 17 km) were arbitrarily assigned values of 17 km. Our final results, represented by the over 700 cases analyzed provide the best data from which further characterization of these techniques can take place.

4. CONTRAIL EXPERIMENT SUPPORT

An extensive data collection campaign was conducted between 18-29 September 1995 as part of a PL/GPA sponsored contrail experiment designed to develop and improve contrail prediction and forecast capabilities. Program objectives are: 1) to determine the vertical and horizontal extent of water vapor from 300-700 mb using an extensive network of airborne, space-based and land-based sensors; 2) test and verify variations of Appleman's equation for contrail formation using real-time data; and 3) use the regional MM5 model to attempt to accurately forecast contrail formation through upper-level moisture enhancements. Ground-based TPQ-11 radar data, satellite observations, and standard 00 and 12 UTC upper air NWS soundings were collected in the vicinity of Hanscom AFB on a daily basis. In addition, a series of radiosonde releases from five surrounding locations was conducted to provide a data rich environment of upper air observations over the contrail experiment area. Radiosonde launches occurred approximately every three hours during daylight hours. The five stations that made up the local radiosonde network were: Hanscom AFB, Beverly, UMASS Lowell, Otis AFB, and Chatham on Cape Cod.

The data-reduction effort was complicated by numerous problems and inconsistencies with the radiosonde measurements that needed to be resolved in order to produce a useful data set. Record books of balloon-flight problems, cloud types and heights as well as technical problems and observations of actual aircraft contrails were used to help classify problems. All radiosonde measurements were subjected to an extensive quality control procedure to identify and remove invalid data. All QC processing was performed manually using a spread sheet program to store and manipulate the data and graphical representations to identify problems in the data set.

4.1 DATA PROBLEMS

Two different manufactures were used to supply radiosondes, VIZ and Vaisala, for the measurement campaign. Throughout the data collection period sondes from the different sources were found to have different sensitivities to relative humidity (RH). The RH of the Vaisala sondes generally ranged between 0 and 80% with very large negative RH values occurring above 400 mb. VIZ sondes were tended to be much less sensitive with a range of RH values typically between 20% and 60%. Often, even with synoptic observations and other supporting meteorological data which confirmed RH values near 100%, VIZ sondes rarely exceeded 60% RH.

Beverly sounding data were noisy relative to the other four sites due to less sensitive receiving equipment and proximity of the site to the FAA tower at Beverly Airport. RF transmitting equipment in the FAA towers severely degraded the quality of signal received by the radiosonde ground system. The parameter most affected was pressure. Contaminated pressure soundings exhibited sinusoidal variations of 0.0 to 0.5 mb about what would be a typical pressure sounding; thus, the pressure parameter required additional processing. Pressure data were smoothed using a running average computed over the six data points above and below the target data point. The smoothing successfully removed the sinusoidal variations.

Because of the proximity of the UMASS Lowell and Beverly sites, and identical release times, some data contamination occurred from the UMASS radiosonde at the Beverly site. During several of the launches, the UMASS sonde was tracked at the Beverly site; sometimes even switching from one radiosonde to another during the tracking period. Difficulty in determining the accuracy and validity of several parameters including pressure, temperature and RH was evident.

Additional processing for the Chatham soundings was needed to account for an incorrect conversion for relative humidity, especially at low (<20%) and high (>95%) humidity values.

4.2 RESOLUTION OF RADIOSONDE PROBLEMS

Radiosonde data from Otis and Hanscom proved to be the most reliable and accurate when pressure, temperature, and RH values were checked against NWS radiosonde sites and other independent data. Significant problems occurred with the UMASS Lowell site and especially with the Beverly data. Figure 17 represents typical pressure related problems with the Beverly data. Approximately the first 900 seconds of data collection occurred before balloon release while the sonde was held on the ground (a common problem). These times were truncated and the start times reestablished from the actual release time. Also, outlying pressure data observable in Figures 17 and 18 were manually removed from the data. Pressure data were then smooothed using a running average of six data points above and below each data point. The radiosonde sounding from Beverly shown in Figure 18 also shows the impact of the UMASS Lowell radiosonde on Beverly's tracking. Near 800 mb and again between 300 and 200 mb contact with the Beverly sonde is lost and the UMASS Lowell sonde is picked up in its place. Soundings of this type were either totally or partially disguarded if the data could not be verified as coming from the Beverly sonde.

Relative humidity proved to be equally difficult as RH values fluctuated greatly over short periods of time, uncharacteristic of actual atmospheric conditions. Large spikes of both positive and negative RH values above 300 mb were common. The Beverly data from 9/22/95 shown in Figure 19 illustrates a typical RH profile. Outlying relative humidity values and fluctuations over short periods were manually removed and negative values set to either 0 or missing (-999). RH values were then smoothed using the six-point running average technique described above.

Some sites such as Beverly provided a limited data set consisting only of pressure, temperature and relative humidity. Other sites also provided dewpoint, corrected RH, wind speed and direction. A common data base was required for the project, so limited data sets were augmented, where possible, with derived parameters to fill in the missing quantities.

27
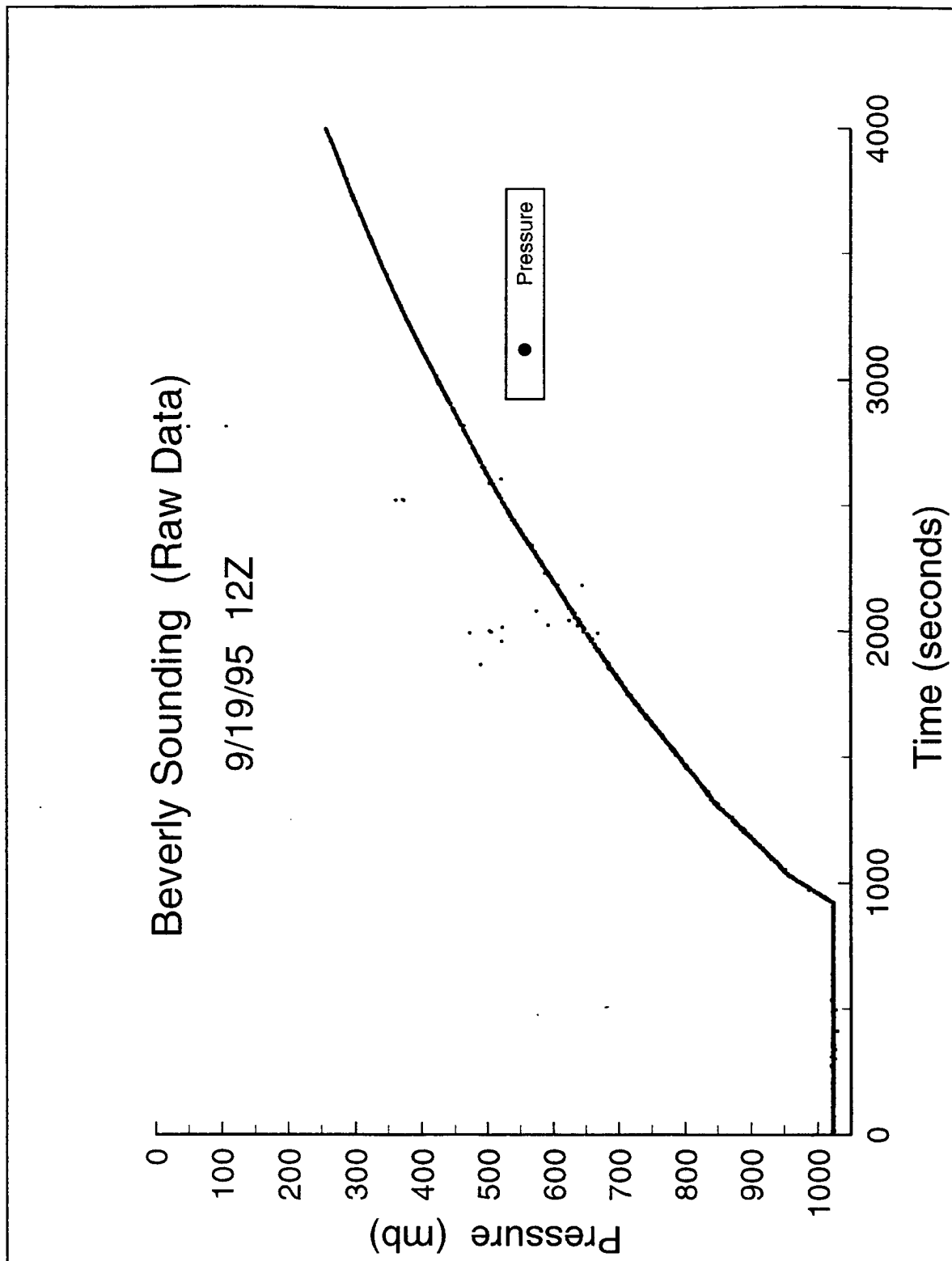
Figure 17. Pressure trace from Beverly sounding, 19 Sep 95 at 1200 UTC. Note constant pressure trace at the beginning of the data collection, prior to balloon release and scatter of data points between 2000 and 3000 seconds.
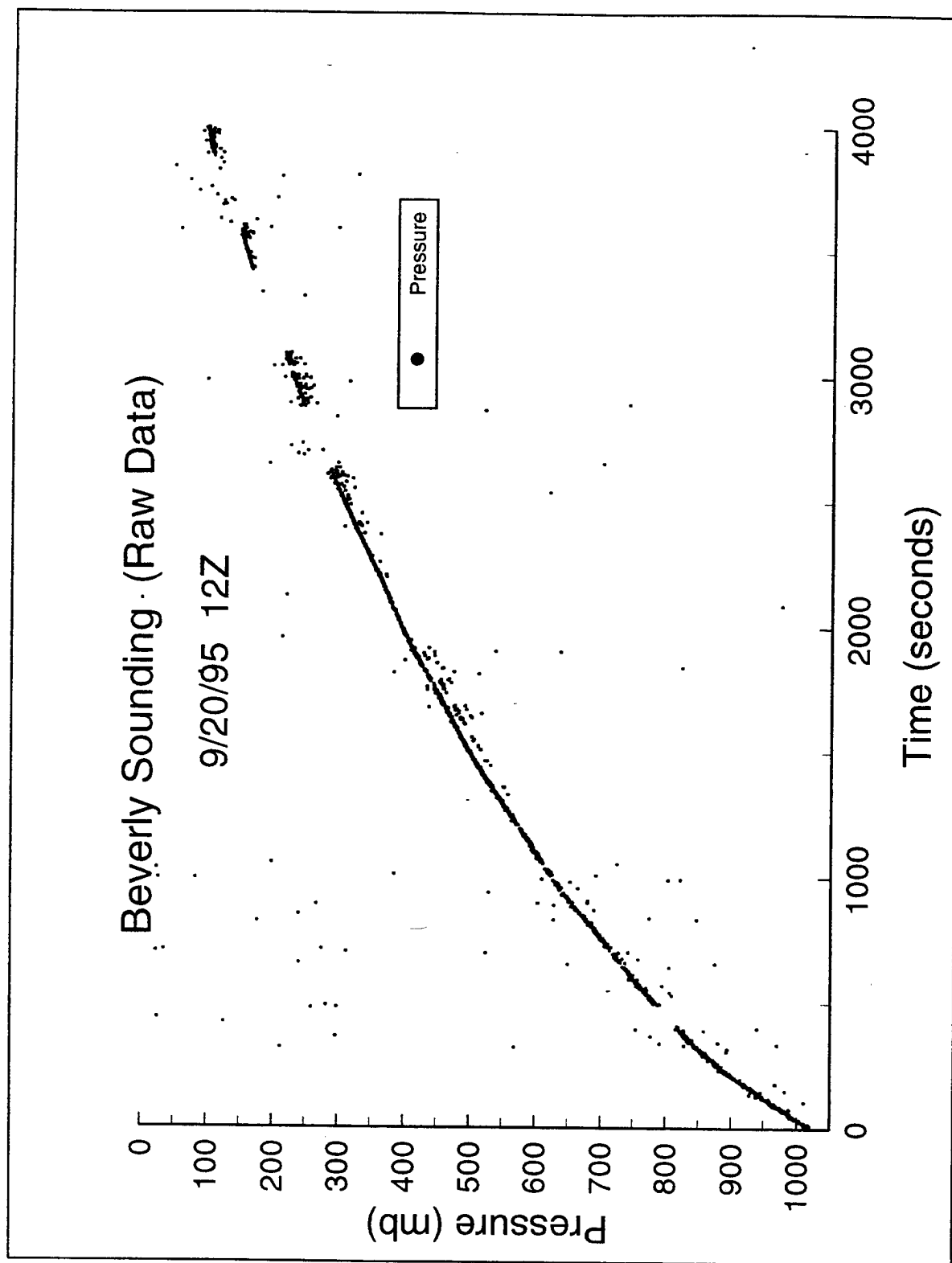
Figure 18. Pressure trace from Beverly sounding, 20 Sep 95 at 1200 UTC. Note scatter and outlying points which were manually removed and then smoothed. Also note data gaps caused by interference with the UMASS Lowell sonde.
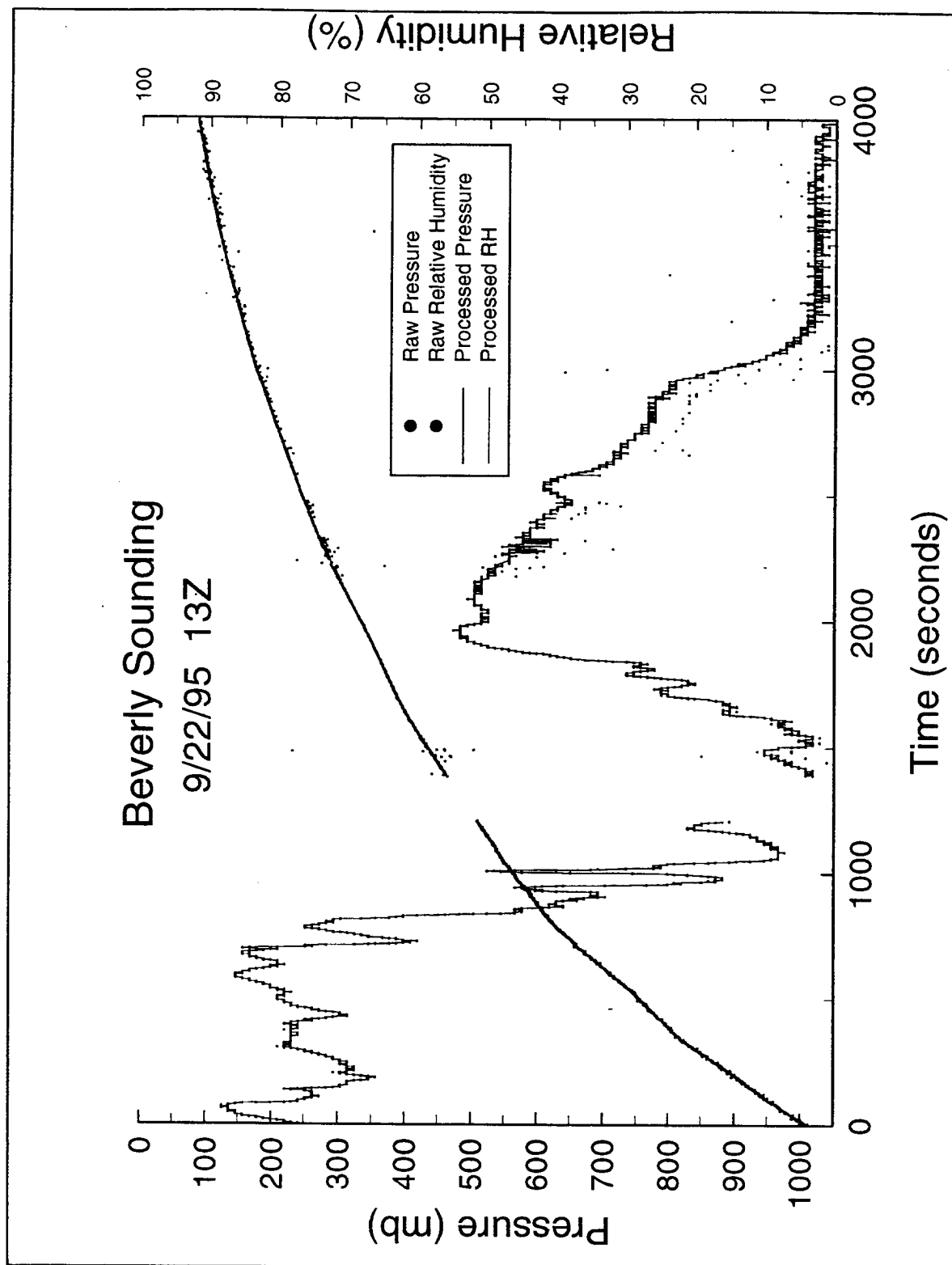
Figure 19. Pressure and relative humidity trace from Beverly sounding on 22 Sep 95, 1300 UTC. Note outlying values in the humidity trace that were manually removed. Also note the break in the sounding between 1200 and 1400 seconds due to interference with UMASS Lowell.

Required parameters were: time since launch, pressure, geopotential height, air temperature, dew point temperature, relative humidity, corrected relative humidity, wind speed, wind direction, distance from launch point. Finally, tropopause height was estimated by manually determining the level of greatest minimum temperature, identifying an isothermal layer above and a decrease in wind speed with height. A determination of tropopause thickness was also made where data permitted. Table 1 is an excerpt from a complete and corrected sounding.

Table 1. Sample Sounding Data from Chatham, MA 1200 UTC 18 Sep 95, After Reformatting and Quality Control Processing

TIME (s)	P (mb)	HT (m)	T (C)	Td (C)	RH (%)	RHc (%)	SPD (m/s)	DIR	X (km)	Y (km)
636	732.8	2675	6.3	-8.4	45.2	0	13.8	296	3.01	-4.96
642	730.6	2700	6.1	-8.3	45.9	0	13.9	295	3.09	-5
648	728.4	2724	5.8	-8.3	46.7	0	14	295	3.17	-5.03
654	726.1	2750	5.6	-7.6	49.1	0	14	294	3.24	-5.07
660	723.9	2775	5.3	-7.6	49.8	0	14	293	3.32	-5.1
666	721.4	2803	5.1	-7.6	50.4	0	14	292	3.4	-5.13
672	719	2830	5	-8.1	49.1	0	13.9	292	3.48	-5.16
678	716.6	2858	4.9	-8.5	48.3	0	13.7	291	3.55	-5.19
684	714.2	2885	4.7	-9.8	45.3	0	13.5	291	3.63	-5.22
690	711.9	2911	4.6	-9.9	45.2	0	13.2	290	3.7	-5.25
696	709.6	2938	4.4	-11.1	42.6	0	12.9	290	3.77	-5.27
702	707.4	2963	4.6	-24.9	19	-0.9	12.6	289	3.85	-5.3
708	705.1	2989	4.8	-75.2	14	-13.7	12.3	289	3.92	-5.32
714	702.9	3015	5	-85.4	11.4	-11.3	12	289	3.98	-5.35
720	700.8	3039	5.2	-85.3	10.9	-10.8	11.7	288	4.05	-5.37
726	698.7	3064	5.4	-85.2	9.9	-9.8	11.5	288	4.12	-5.39
732	696.6	3088	5.6	-85.2	9.2	-9.1	11.3	287	4.18	-5.41
738	694.5	3113	5.8	-85.1	9.3	-9.2	11.1	287	4.25	-5.43
744	692.4	3138	6	-85	9.2	-9.1	10.9	287	4.31	-5.45
750	690.2	3164	6.2	-84.9	9.3	-9.2	10.8	286	4.37	-5.46

4.3 SUMMARY

Radiosonde data collected as part of the PL/GPA Contrail Experiment required considerable manual quality control and editing as part of the data reduction process. This process is summarized in the steps below:

1 Bad data were manually edited to remove obviously incorrect data and replace them with a missing designation. This was accomplished by plotting the sounding and manually identifying bad data points.

2 Additional editing of Beverly radiosonde data was required. Beverly data were noisier than sounding data from the other four sites due to less sensitive ground-receiving equipment and the proximity of the site to the FAA control tower. The parameters most affected were pressure and RH. Bad data were corrected where possible and then smoothed using a running six-point average.

3 Additional processing for Chatham soundings was needed to correct for RH extremes. This was accomplished by Steve Williams of UCAR.

4 Missing layers were noted.

5 Corrections for launch times were noted.

6 Vertical coverage of each sounding was noted.

7 The subjective quality assessment for each sounding was recorded (e.g., was the same radiosonde being tracked during the flight).

8 Each sounding tagged by the sonde manufacturer, either VIZ or Vaisala.

9 Tropopause height and thickness determined if possible.

10 A common format for all radiosonde soundings was established and missing parameters calculated.

11 All radiosonde data archived in a common format.

5. AIMS DEVELOPMENT

The Air Force Interactive Meteorological System (AIMS) is an integrated system composed of general-purpose and function-specific processors developed originally to support research in remote sensing, principally satellite meteorology. AIMS is jointly operated and maintained by PL/GPA and AER under a Cooperative Research and Development Agreement (CRADA). The current configuration of AIMS is summarized in Table 2 and illustrated by the schematic in Figure 20. AIMS consists of DEC VAX and Alpha minicomputers, a SUN compute server, two Silicon Graphics (SGI) imaging workstations, two imaging workstations built around Adage image processing systems, GOES-8/9, NOAA/TIROS, DMSP, and METEOSAT-5 ground stations interfaced to SUN workstations, and desktop NCD color X-terminals.

AIMS satisfies the needs of some twenty active users through four functional capabilities: network access; real-time and archived data sources; data visualization and image processing; and interactive and batch processing. Ethernet hardware provides the network backbone for AIMS, all systems are either tied directly to the AIMS Ethernet or are reachable through a network gateway computer. Local Area VMScluster (LAVC) software tightly couples all DEC VAX and Alpha processors, providing transparent access to remote file systems and print and batch queue facilities. The UNIX-based platforms (SGI and SUN) share data directly using SUN Microsystems Network File System (NFS) while a third-party implementation of NFS, known as MultiNET, allows select VAX and Alpha processors to participate in the local-area network as an NFS clients and servers. The GP network links the AIMS to numerous outside networks via an Ethernet bridge. Outside
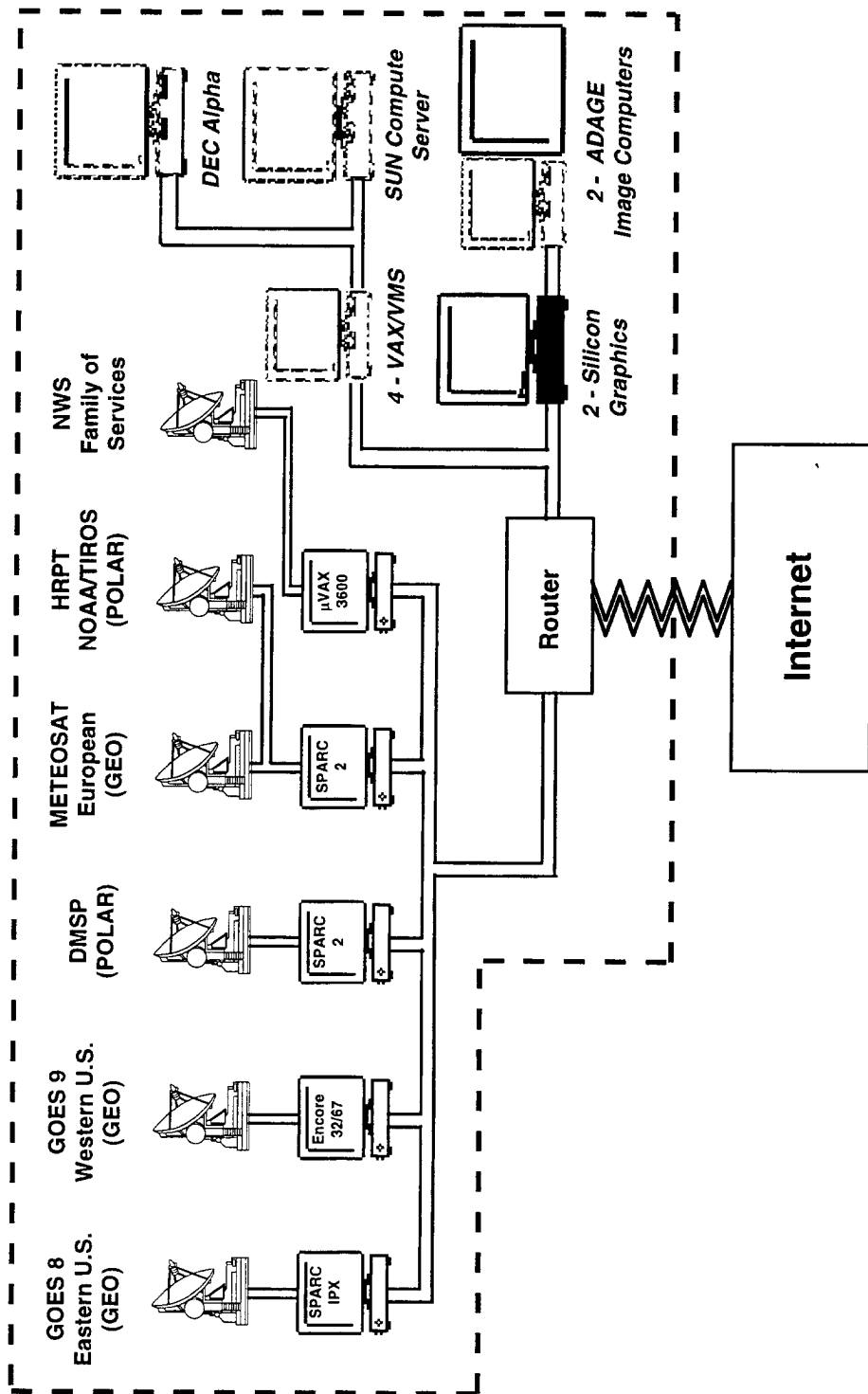
Figure 20. AIMS system configuration.

33

Table 2. Physical and Functional Overview of AIMS

Qty	System	O.S.	Memory (MB)	Disk (MB)	Tape	Description
1	Sun Sparc 20	UNIX	64	7000	8mm	GOES-8/9 realtime ingest
1	Sun Sparc II	UNIX	64	3000	4mm	NOAA/HRPT realtime ingest
1	Sun Sparc II	UNIX	64	2400	4mm	DMSP/RTD realtime ingest
1	Sun Sparc IPX	UNIX	64	5000	4mm	METEOSAT-5 realtime ingest
2	Adage 3000		4-16			Image processing/display
2	VAXstation 3600	VMS	16	70	TK50	Adage host, 8-bit display
2	Silicon Graphics Indigo^2 Extreme	UNIX	96	3000		Image processing/display
14	NCD X-Terminals	X11	14			Desktop 8-bit image display Host and local services
1	Micron PC	W/NT	64	4000	8mm 1/4	Intranet Documentation Server
1	Micron PC	W/95	64	6000	1/4	CD-ROM server
1	AlphaServer 2000	VMS	256	8000	8mm	Oracle database server
1	Sun Enterprise 2	UNIX	576	12000	8mm	Compute server
1	VAX 4000-105A	VMS	128	5500 1300 (2)		X-Terminal server Removable optical media NFS client/server
2	VAX 4000-100	VMS	128	4200 1300	8mm	X-Terminal server Removable optical media NFS client/server Interactive/Batch processing
1	VAXstation 4060	VMS	72	2500 1300 (3)		8-bit image display Weather data ingest Optical server
1	VAXserver 3800	VMS	32	1050 1300	8mm 9-track	Boot server Removable optical media

networks including NSI, DDN, and NEARnet (DDN and NEARnet are both members of Internet) provide access to laboratories, government facilities, and private companies world wide. AIMS also has access to a direct T1 satellite link between the Geophysics Directorate at Hanscom AFB and a Cray-2 supercomputer at Kirtland AFB, NM.

Meteorological and supporting data flow into AIMS through several possible routes: 1) real-time direct broadcast satellite transmissions, 2) direct serial links, 3) 9 track, 8mm, or 4mm DAT magnetic tape, 4) network file transfers (e.g., FTP), or 5) CD ROM optical disks. Satellite transmissions are received directly at one of four satellite ground stations configured to receive GOES, NOAA/HRPT, METEOSAT, and DMSP broadcasts. Table 3 summarizes the characteristics of the sensor data routinely ingested by these systems and

Table 3. Characteristics of Satellite Sensor Data Used on AIMS

Satellite/ Channel	Instrument Wavelength or Frequency (μm) (GHz)	Resolution at Nadir (km)
DMSP OLS		
Visible	0.4 - 1.1 μm	0.6
Longwave IR	10.5 - 12.6 μm	2.8
DMSP SSM/I [1]		
1	19.35 GHz V/H	25
2	22.235 GHz V	25
3	37.0 GHz V/H	25
4	85.5 GHz V/H	12.5
DMSP SSM/T2		
1 (Window)	91.5 GHz	90
2 (H_2O)[2]	150 GHz	64
3 (H_2O)	183 +/- 1 GHz	50
4 (H_2O)	183 +/- 3 GHz	50
5 (H_2O)	183 +/- 7 GHz	50
NOAA AVHRR		
Visible/Near IR	0.58 - 0.68 μm	1.1, 4[3]
Visible/Near IR	0.725 - 1.1 μm	1.1, 4[3]
Shortwave IR	3.55 - 3.93 μm	1.1, 4[3]
Longwave IR	10.3 - 11.3 μm	1.1, 4[3]
Longwave IR	11.5 - 12.5 μm	1.1, 4[3]
NOAA HIRS		
1 - 7 (CO_2/H_2O)	13.3, 13.6, 13.9, 14.2, 14.4, 14.7, 14.9 μm	42
8 (Window)	11.11 μm	42
9 (O_2)	9.71 μm	42
10 - 12 (H_2O)	6.72, 7.33, 8.22 μm	42
13 - 17 (N_2O/CO_2)	4.23, 4.40, 4.46, 4.52, 4.57 μm	42
18 - 19 (Window)	3.76, 4.00 μm	42
20 (Window)	0.69 μm	42
NOAA MSU		
1 (Window)	50.31 GHz	168
2 (O_2)	53.74 GHz	168
3 (O_2)	54.96 GHz	168
4 (O_2)	57.95 GHz	168
NOAA SSU		
1 (CO_2)	15.0 μm	62
2 (CO_2)	15.0 μm	62
3 (CO_2)	15.0 μm	62
GOES Imager		
1	0.55 - 0.75 μm	1
2	3.8 - 4.0 μm	4
3	6.5 - 7.0 μm	8
4	10.2 - 11.2 μm	4
5	11.5 - 12.5 μm	4

GOES Sounder

1	14.71 μm	8
2	14.37 μm	8
3	14.06 μm	8
4	13.64 μm	8
5	13.37 μm	8
6	12.66 μm	8
7	12.02 μm	8
8	11.03 μm	8
9	9.71 μm	8
10	7.43 μm	8
11	7.02 μm	8
12	6.51 μm	8
13	4.57 μm	8
14	4.52 μm	8
15	4.45 μm	8
16	4.13 μm	8
17	3.98 μm	8
18	3.74 μm	8
19	0.70 μm	1

Meteosat

1	0.5 - 0.9 μm	2.5
2	5.7 - 7.1 μm	5
3	10.5 - 12.5 μm	5

[1]Channel data are dual polarized except 22.235 GHz which are only vertically polarized.

[2]Principal absorbing constituents for sounding channels.

[3]Nominal resolution for all channels is 1.1km. GAC data are available at 4km reduced resolution.

Figures 21 and 22 show the direct-broadcast coverage for the geostationary and polar-orbiting platforms respectively. Because the ground stations are based around non-DEC computers, the MULTINET software is required to provide the AIMS LAVC transparent access to the data. GOES, NOAA/HRPT, METEOSAT and DMSP ground station computers maintain a comprehensive third-party software package known as Terascan used to extract, format, calibrate, and Earth-locate subsets of the telemetry data. X11 windows-based software is also provided for interactive image display and processing of the data. All routinely scheduled data ingest events from the four groundstations are archived either to 4mm or 8mm tape. Table 4 summarizes the local coverage satellite data archive on AIMS.

Conventional meteorological data are used extensively on AIMS to support a wide range of applications. These data are made available via serial connections to two components of the National Weather Service (NWS) Family of Services. The first component, known as the Domestic Data Service (DDS), provides coded observations, reports, forecasts, and analyses for the U.S., Canada, and the Caribbean. The second component is known as the International Data Service (IDS) and provides worldwide coded observations, reports, and forecasts. The Family of Services multiplexes data originating
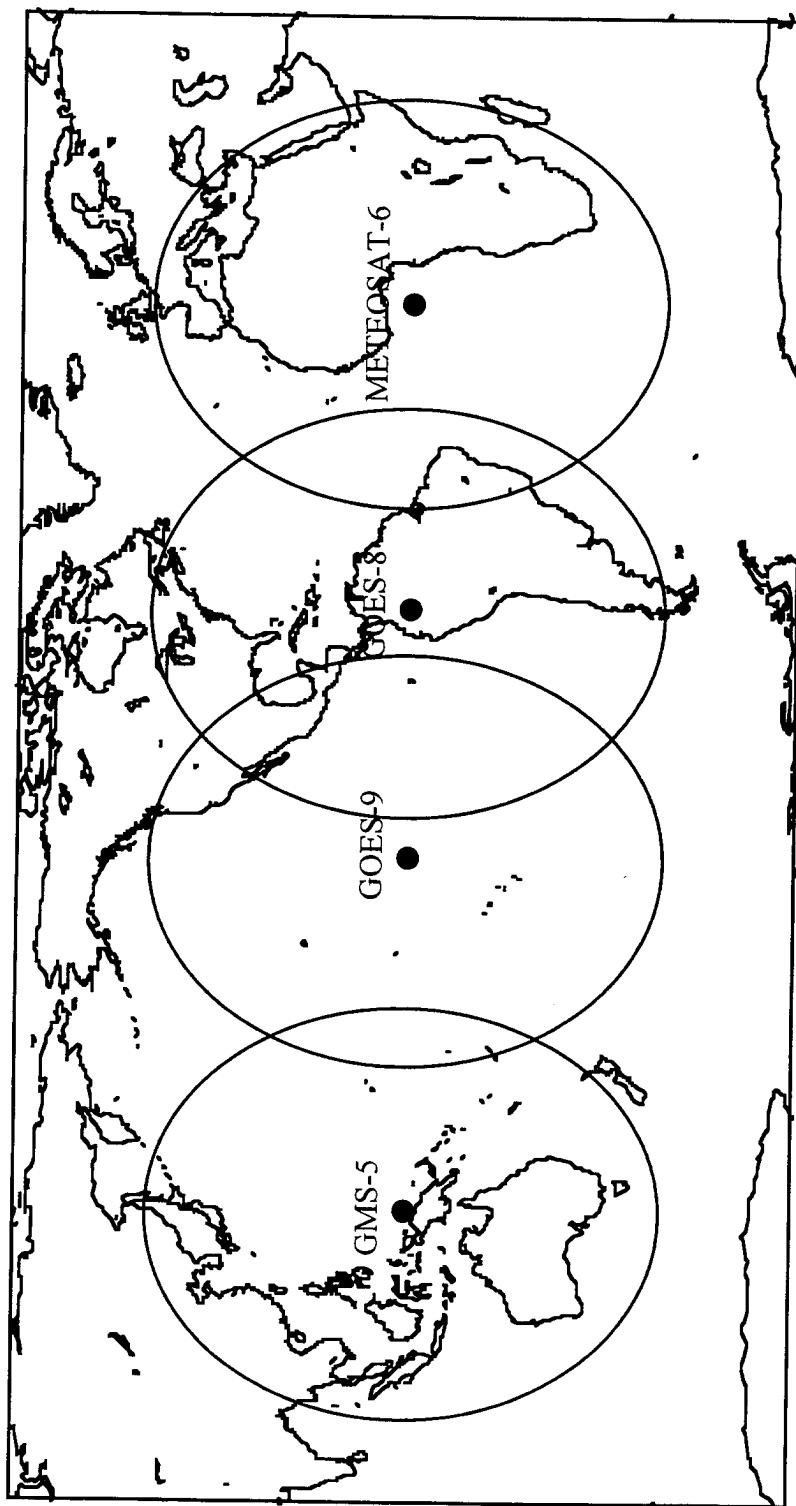
Figure 21. Data coverage from the GOES 8 satellite direct-broadcast transmissions acquired in real-time by the AIMS geostationary ground stations.
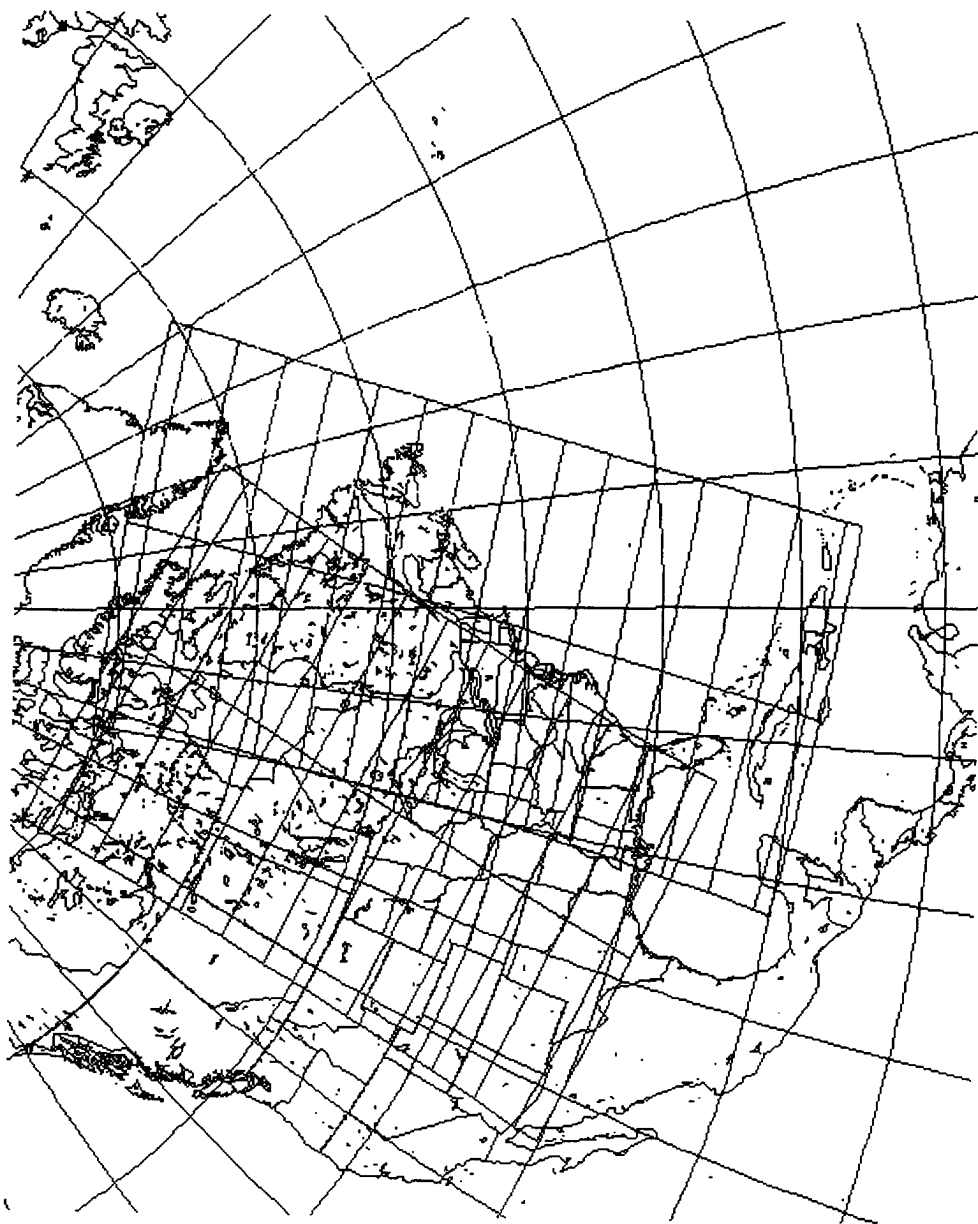
Figure 22. Data coverage from NOAA polar-orbiting satellite direct-broadcast transmissions acquired in real-time by the AIMS HRPT ground station.

Table 4. Local Coverage Satellite Data Archive

Platform	Dates
NOAA/HRPT[1]	22-Sep-92 - present
DMSP/RTD[2]	1-Sep-93 - present
GOES-8	28-Jul-95 - present
Meteosat-4/5	15-Sep-93 - present

[1] Satellites NOAA 11, 12, and 14.
[2] Satellites F-11 and F-12.

from different sources, producing a data stream of point, gridded, and tabular data with varied formats. AIMS recognizes, decodes and reformats a subset of data sources that includes Service A, synoptic, ship and buoy, METAR, upper-air, manually digitized radar (MDR), and NMC model guidance. Table 5 describes the conventional meteorological data sources available on AIMS. All data have been archived to 8mm tape since September of 1989.

Table 5. Conventional Meteorological Data Sources Available on AIMS

Source	Type	Coverage	Frequency	Data Characteristics
Service A[1]	Point	U.S., Canada	Hourly	Surface observations
Synoptic	Point	Global	4/8 times daily	Surface observations
METAR	Point	Global	8 times daily	Surface observations
Ships/Buoys	Point	Global	4/8 times daily	Platform observations
Upper Air	Point	Global	Twice daily	Radiosonde, rawinsonde measurements
Forecast Guidance	Point	U.S.	Twice daily	ETA and NGM model output. Forecasts for 6 hour intervals out to 48 hours
Forecast Model Output Statistics (MOS)	Point	U.S.	Twice daily	Statistically-based forecasts derived from the models. Forecasts for 6 hour intervals out to 48 hours
Trajectory Forecasts	Point	U.S.	Twice daily	Statistically-based forecasts derived from the models. Includes parcel trajectories for 6 hour intervals out to 24 hours
Manually Digitized Radar (MDR)	Gridded	U.S.	Hourly (on the half-hour)	Maximum reflectivity reported for grid box. Also station status and some cell characteristics

[1] On July 1, 1996 the Service A format was changed to METAR format.

39

Data on magnetic tape are received from numerous outside agencies including AFGWC, ETAC, NOAA/NESDIS, NASA, NCAR, ASL and GMGO. Historically, tapes have been the preferred method for transferring data from outside the organization, however, this is rapidly being replaced by direct file transfers via Internet. Recently, the Defense Mapping Agency began distributing large volume geographic data sets on CD ROM. CD ROM is also becoming the preferred medium for software vendors to distribute new and revised software packages to customers.

Most network file transfers from outside the laboratory enter the system via a separate gateway computer maintained by the Geophysics Directorate's main computing center. This gateway computer is a node on the GP network and communicates with AIMS using various protocols, most notably the TCP/IP protocol.

Satellite data dominate all other data types in competition for system resources. A primary system design consideration for AIMS was effective management of the vast amount of imager and sounder data available from the satellite sensors (see Table 3) as well as products derived from the raw data (e.g., algorithm development for cloud analysis and forecasts). To this end, a DEC Alpha running the Oracle Server, a networked-based relational database management system, was configured to facilitate management and user access to the vast amount of archived and online satellite data. AIMS currently supports 64GB of fixed disk mass storage as well as rewritable optical disk drives that provide 1.3GB of storage per cartridge. With 9 optical drives currently configured on AIMS, 5.4GB of data can be made immediately available at any one time. Fixed disk mass storage is routinely backed-up to 8mm tape.

Visualization of data and experiment results is probably the single most important capability on AIMS. Virtually every scientific project that uses AIMS exploits this capability, at least for quality control of the input data and validation of algorithm results. There are basically three types of display systems on AIMS. The first are image processing workstations that consist of VAXstation 3600 single user systems linked to Adage 3000 imaging subsystems. Each workstation configuration consists of two monitors, one each for the VAXstation and the Adage, large frame buffers, high speed bit-slice processors for processing raster data, multiple 8-bit look up tables, and keyboard and mouse for user input. These systems are capable of performing standard image processing and display functions on large multispectral data sets at interactive speeds. The VAXstation and Adage subsystems complement each other functionally with the VAXstation providing network communications, a standardized user interface, and high level graphical display capabilities while the Adage provides high speed display and image manipulation functions. The second type comes from the two SGI Indigo 2 Extreme imaging workstations. These workstations extend the visualization capabilities of AIMS through a high performance RISC-based workstation capable of real-time 2- and 3-D graphics and imaging that can be implemented using standards such as the X Windows system for 2-D applications and OpenGL for 3-D graphics and imaging. The SGI systems have 96MB of system memory that doubles as pseudo frame buffer memory and a 2GB hard disk for image storage. Vendor supplied software includes Explorer, interactive visualization software for 2- and 3-D applications and ImageVision, an object-oriented library used to create, process, and display imagery. Recent work has focused efforts to port much needed Adage application functionality to the SGI systems due to ever increasing chances of an Adage failure and the lack of spare parts (the Adages are 14 years old). The third type of display system available on AIMS are desktop color X-terminals. These systems are characterized by 8-bit color graphics, ample system memory, and host services provided by SUN, SGI, or DEC platforms. They provide an X window based interface to AIMS, support local clients including TELNET, CTERM and LAT services, generally reside within individual offices and are used for a variety of applications including software development, analysis and

display of meteorological data, word processing, network communications, and other general purpose computing. X windows is the *de facto* interface standard for all AIMS workstations due to its functionality and nearly universal acceptance across hardware platforms.

Although AIMS was primarily developed to support interactive computing there has been a consistent secondary need to support relatively compute-intensive jobs through batch processing. All VMS systems have batch queues as an integral part of the operating system, however, on AIMS a select number of systems have been tailored to handle relatively large batch type operations. To satisfy the requirement for batch capabilities in an efficient manner, several system wide batch queues have been developed. Each queue is matched to a particular type of application depending on the requirements for memory, mass storage, CPU, and wall clock time. Each queue is backed by system resources designed to provide optimal performance for its particular type of application with minimal impact on the rest of the cluster. More recently, a SUN Enterprise 2 multi-processor server was purchased to provide ever-increasing compute-intensive processing being conducted on UNIX platforms.

Software has been developed on AIMS to perform standard display operations for satellite imagery such as greyshade imaging, pseudo color enhancements, time-series looping and graphical display. Also, the Adage and SGI systems support full color display of multispectral imagery as well as fast interactive image enhancement and filtering operations. The Image Vision library contains a core set of image processing functions that include color conversion, arithmetic functions, radiometric and geometric transforms, statistics, spatial and non-spatial domain transforms, and edge, line, and spot detection. For conventional meteorological data a substantial number of applications have been developed to facilitate access to and processing of these data. General purpose list, plot, and contour applications are available for use. Data access methods supported by these applications include time-series for a single station; geographic retrievals by station list, political boundary, latitude-longitude box, or user-defined keyword; and compound retrievals for data fusion applications. For applications development AIMS supports the C, C++, and FORTRAN languages for 3GL programs; IDL, GKS, NCAR Graphics, MOTIF/X11, Explorer, OpenGL, and ImageVision for graphics and imaging and X-Designer for building graphical users interfaces.

Other resources available on AIMS include a dial-in capability (2 lines), black and white and color laser printers and a high-quality color printer based on dye-sublimation technology suitable for producing publication-quality hardcopy output. A Pentium-based PC running the Windows NT-Server operating system acts as an Intranet documentation server, providing documentation for programmed applications and libraries, computer-related procedural tasks (e.g. how to restore selected archives), and file format descriptions to name a few. Users seeking documentation will be able to use a web browser to query and locate specific documentation from the server. A second Pentium-based PC hosts a CD-ROM Recorder for creating CD-ROMS and a 2GB user disk to stage recording data. The PC is networked so that users can transfer data from any AIMS node to the staging disk using FTP or NFS.

6. REFERENCES

Atzeni, P. and V. De Antonellis, 1993: Relational Database Theory. Benjamin Cummings Publishing Co., 389 pp.

Barton, I.J., 1983: Upper Level Cloud Climatology from an Orbiting Satellite. Journ. Atmos. Sci., 40, 435 - 447.

Chen, P.P. (Editor), 1983: Entity-Relationship Approach to Information Modeling and Analysis. North-Holland, Amsterdam, the Netherlands.

d'Entremont, R.P., D.P. Wylie, S.-C. Ou, and K.-N. Liou, 1996: Retrieval of Cirrus Radiative and Spatial Properties Using Coincident Multispectral Imager and Sounder Data. Preprints, Eighth Conf. on Satellite Meteorology and Oceanography, Amer. Meteor. Soc., Atlanta, GA, 28 January - 2 February 1996, 377 - 381.

d'Entremont, R.P., D.P. Wylie, D.C. Peduzzi, and J. Doherty, 1993: Retrieval of Cirrus Radiative and Spatial Properties Using Coincident AVHRR and HIRS Satellite Data. Proceedings, Passive Infrared Remote Sensing of Clouds and the Atmosphere. SPIE - The Int'l. Soc. for Optical Engineering, 1934, 13-15 April 1993, Orlando, FL (in press).

d'Entremont, R.P., D.P. Wylie, J.W. Snow, M.K. Griffin, and J.T. Bunting, 1992: Retrieval of Cirrus Radiative and Spatial Properties Using Independent Satellite Data Analysis Techniques. Proceedings, Sixth Conference on Satellite Meteorology and Oceanography, Amer. Meteor. Soc., 5-10 January 1992, Atlanta, GA, 17 - 20.

d'Entremont, R.P., M. K. Griffin, and J. T. Bunting, 1990: Retrieval of Cirrus Radiative Properties and Altitudes Using Multichannel Infrared Data. Proceedings, Fifth Conference on Satellite Meteorology and Oceanography, Amer. Meteor. Soc., 3-7 September 1990, London, England, 4-9.

Gustafson, G.B., R.G. Isaacs, R.P. d'Entremont, J.M. Sparrow, T.M. Hamill, C. Grassotti, D.W. Johnson, C.P. Sarkisian, D.C. Peduzzi, B.T. Pearson, V.D. Jakabhazy, J.S. Belfiore, and A.S. Lisa, 1994: Support of Environmental Requirements for Cloud Analysis and Archive (SERCAA): Algorithm Descriptions. PL-TR-94-2114, Phillips Laboratory, Hanscom AFB, MA, ADA283240.

Hoke, J.E., J.L. Hayes, L.G. Renninger, 1981: Map projections and grid systems for meteorological applications. AFGWC-TN-79-003, Air Weather Service, Scott AFB, IL.

Hunt, G.E., 1973: Radiative Properties of Terrestrial Clouds at Visible and Infra-Red Thermal Window Wavelengths. Quart. Journ. Royal Meteor. Soc., 99, 346 - 369.

Ingram, W.J., 1989: Modeling Cloud Feedbacks on Climate Change. Weather, 44, 303 - 311.

Menzel, W.P., D.P. Wylie, and K.I. Strabala, 1992: Seasonal and Diurnal Changes in Cirrus Clouds as Seen in Four Years of Observations with the VAS. Journ. Appl. Meteor., 31, 370 - 385.

Ou, S.C., K.N. Liou, W.M. Gooch, and Y. Takano, 1993: Remote Sensing of Cirrus Cloud Parameters Using AVHRR 3.7 and 10.9 mm Channels. Appl. Optics, April 1993 (in press).

Parol, F., J.C. Bruiz, G. Brogniez, and Y. Fouquart, 1991: Information Content of AVHRR Channels 4 and 5 with respect to the Effective Radius of Cirrus Cloud Particles. Journ. Appl. Meteor., 30, 973 - 984.

Schiffer, R.A., and W.B. Rossow, 1983: The International Satellite Cloud Climatology Project(ISCCP): the First Project of the World Climate Research Programme. Bull. Amer. Meteor. Soc., 64, 779 - 784.

Smith, W.L., H.E. Revercomb, H.B. Howell, and M.-X. Lin, 1990: Multi-spectral Window Radiance Observations of Cirrus From Satellite and Aircraft, November 2, 1986 Project FIRE. FIRE Science Results 1988, NASA Langley Res. Ctr., 89 - 93.

Takano, Y., and K.N. Liou, 1989: Solar Radiative Transfer in Cirrus Clouds. Part I: Single Scattering and Optical Properties of Hexagonal Ice Crystals. Journ. Atmos. Sci., 46, 3 - 19.

Woodbury, G.E., and M.P. McCormick, 1983: Global Distribution of Cirrus Clouds Determined from SAGE Data. Geophys. Res. Lett., 10, 1180 - 1183.

Wylie, D.P., and W.P. Menzel, 1989: Two Years of Cloud Cover Statistics Using VAS. Journ. of Clim., 2, 380 - 392.

APPENDIX A

DATA SAVE DOCUMENTATION REPORT
for
SBIRS Phenomenology Exploitation Project

A-1.0 Introduction

This Data Documentation Report provides a description of the first data save made for the Space Based Infrared Systems (SBIRS) project. It provides a description of the data set, its format, how it was gathered and processed, and a description of the algorithms used to generate it. The data set consists of analyzed products produced by the SERCAA cloud property retrieval algorithms. The period covered is 1 August - 30 September 1995 for the SBIRS region of interest: Eastern United States. All available data from the AIMS satellite ground stations for those dates are included. Data were analyzed specifically for SBIRS using software developed from the SERCAA cloud analysis algorithms described by Gustafson et al. (1994) and subsequently modified for SBIRS. Substantial new algorithm development for optical property retrieval were required to accommodate the objectives in processing this data set. Four tapes are provided, each containing partial results.

A-2.0 Processing Environment

Satellite data processing for this data set used the SERCAA cloud analysis algorithms described by Gustafson et al. (1994). Multisource data from the NOAA-12 and NOAA-14, and GOES-8 satellites were used. All data were obtained from the Phillips Laboratory direct readout ground stations and data processing was performed on the Air Force Interactive Meteorological System (AIMS) at the Phillips Laboratory. Two processing levels of the SERCAA cloud analysis algorithms were used as summarized in Figure A-1.
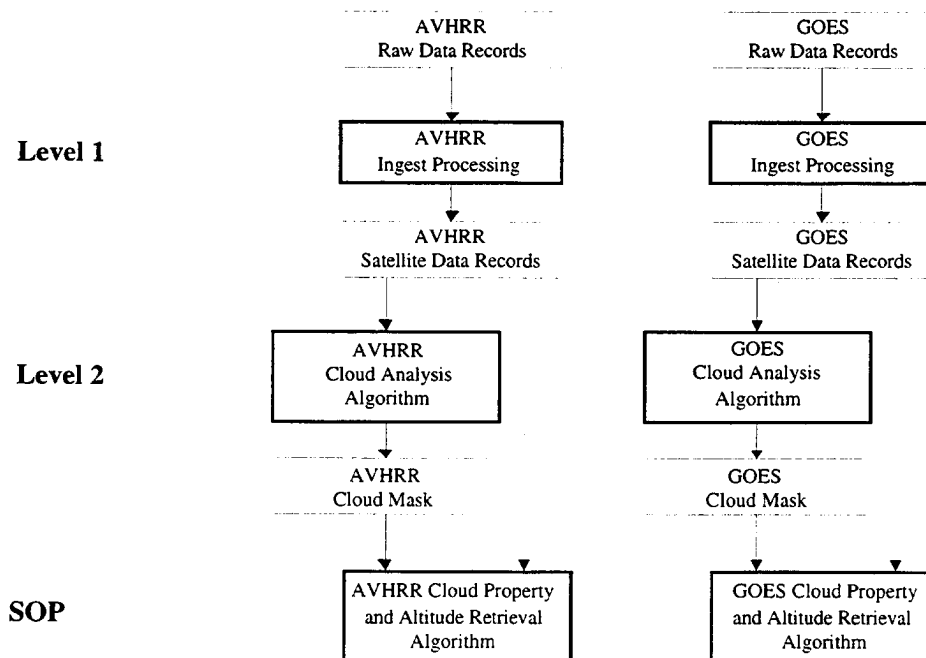
Figure A-1 SBIRS Processing data flow and processing levels

Level 1 processing consists of data ingest. Archived data are processed through separate ingest programs depending on the data source and format. All data are then stored in a standard format in the original satellite-scan projection. The format consists of flat files where the number of elements correspond to the number of pixels in the satellite-scan line and the number of rows corresponds to the number of scan lines. Data are maintained on AIMS through the SERCAA Database (SDB) management software. Level 1 data products

45

consist of separate files for each sensor channel plus two additional files containing Earth location and satellite/solar geometry information. Satellite data characteristics are summarized in Table A-1. The GOES visible data are sub-sampled by a factor of four to match the IR data resolution. Earth location data consist of latitude-longitude pairs that are maintained at a sub-sampled resolution relative to the satellite data. For each sensor scan line, one latitude-longitude pair is provided for every n^{th} pixel, where n varies with satellite. Geometry information is also sub-sampled in the same ratio as the Earth location information and consists of three angles: satellite zenith, solar zenith, and sun-satellite azimuth. Ingest products are described more completely in Section 2 of Gustafson et al. (1994).

Table A-1. Sensor Channel Data Attributes

Satellite	Sensor	Channel (μm)	Data Format	Resolution[1] (km)	Bits per Pixel[2]	Pixels per Scan Line
NOAA	AVHRR	0.58-0.68	percent albedo	4.0	10	409
		0.72-1.10	percent albedo	4.0	10	409
		3.55-3.93	EBBT	4.0	10	409
		10.3-11.3	EBBT	4.0	10	409
		11.5-12.5	EBBT	4.0	10	409
GOES	GVAR	0.55-0.75	percent albedo	1.0	10	20944
		3.8-4.0	EBBT	4.0	10	5236
		6.5-7.0	EBBT	8.0	10	5236
		10.2-11.2	EBBT	4.0	10	5236
		11.5-12.5	EBBT	4.0	10	5236

[1]Sensor resolution at satellite subpoint that will provide global coverage.

[2] Radiance data are transmitted at 10-bit resolution, however, the SERCAA development system could only accommodate 8-bit brightness temperature data (although the full 10-bit resolution is used in the radiance-to-brightness-temperature transformation).

Level 2 processing consists of sensor-specific nephanalysis algorithms. Level 1 sensor data from NOAA and GOES satellites are processed through separate algorithms as indicated in Figure A-1. Each time data from a new satellite pass are ingested, they are analyzed using the appropriate nephanalysis algorithm and results are placed in a Level 2 output file. One output file is generated for each nephanalysis run and nephanalysis results are stored in the original satellite scan projection with one byte of information for each pixel. Each byte is bit-packed according to the map in Table A-2. For each set of Level 1 products generated from a satellite pass, one Level 2 product file is generated.

Table A-2. Cloud Analysis Algorithm MCF File Bit Assignments

Bit	Assignment	Description
0	Cloud Mask	ON = Cloud-Filled OFF = Cloud-Free
1	Low Cloud	ON = Low Cloud Found
2	Thin Cirrus Cloud	ON = Thin Cirrus Cloud Found
3	Precipitating Cloud	ON = Precipitating Cloud Found
4	Partial Cloud	Only used by DMSP algorithm
5	Data Dropout	ON = Missing or Unreliable Data
6	Confidence	0 = Missing Data; 1 = Low;
7	Flag	2 = Middle; 3 = High

SBIRS Optical Property (SOP) Retrieval processing uses Level 1 and 2 products as input to calculate cloud top altitude, pressure and emissivity. It maintains the data in the individual satellite projections and resolutions. Optical property retrieval products are generated for each pixel and contain the information in Table A-3. A maximum of four products can be generated for each pixel. One set of product files is created for each set of Level 1 and 2 products. All products associated with a single satellite pass are related through SDB and are provided on the tapes as a set.

Table A-3. Cloud Property Retrieval Output

Parameter	Description
lat	latitude coordinate for each pixel (in hundredths of a degree)
lon	longitude coordinate for each pixel (in hundredths of a degree)
sdb_entry	SDB entry number of input VIS sensor data
ddd	Sensor data Julian date
hhmm	Sensor data valid time (UTC)
altitude	Cloud top altitude of pixels (in 1/17 km)
pressure	retrieved pressure values for each pixel (mb)
3.7 emissivity	retrieved emissivity at 3.7 μm
10.5 emissivity	retrieved emissivity at 10.0 μm
sunrise	Local sunrise time (UTC)
sunset	Local sunset time (UTC)
vid	Satellite vehicle (platform) ID

A-3.0 Tape Format

All data for the 1 August - 30 September 1995 SBIRS data save are contained on four 8mm tapes written in UNIX tar format. Each tape contains analysis products for multiple days of data but for only on satellite type (i.e., GOES or NOAA). The size of the combined Level 1, 2 and SOP products is approximately 1.1 Gbytes plus approximately 545 Mbytes of geo-location data. In addition to the tapes, hard-copy listings of the contents are also provided. It may be useful to place the listing file into an edit program to scan and search it quickly. The listings are required to locate specific data sets on the tapes. A procedure is outlined in Section 5 for correlating SERCAA Optical Products (SOP) data with other data sets.

SERCAA level 1 and 2 and SBIRS Optical Property products are generated for each new pass of polar-orbiting satellite data and for three-hourly GOES data received during the period of the data save. All available data for the period covered were included; any gaps in the data list are due to either missing or bad data. A few scans had to be dropped from the processing stream due to excessive bad or missing lines. Satellite eclipse periods, when no sunlight reaches the satellite solar panels, occurred in late August and early September and also caused some periodic drop-outs. Typically 3 to 5 hours per day beginning around 0300 UTC were lost during the eclipse period. For data archiving purposes all SBIRS products associated with a given satellite pass were placed in a single directory and subsequently placed on tape. Thus each tape contains a series of several hundred tar files. For each tape, there is also SDB Information, contained in files named either *goes.list* or *avhrr.list*. These files contain descriptive metadata information extracted from the SERCAA database that describe the relevant attributes of the SERCAA product files (e.g.,

number of pixels in a scan line of satellite data and the number of scan lines in the file). Information on sub-sampling ratios for the Earth location and angles files are also contained there.

Detailed descriptions of the file formats used for each output level, and the associated information files, supplied for the 1 August - 30 September 1995 save are provided in Section 4. Section 5 provides a guide for extracting data sets from tape.

A-4.0 Archive Data Format Description

All image files contain fixed-length records. The number of lines and number of elements in an image file are contained in the SDB information file that is provided with the tape, under the heading of *goes.list* or *avhrr.list*:

NUM_LINES   Number of image data lines in the file.
ELEM_PER_LINE   Number of elements (pixels) per line.
BYTES_PER_ELEMENT   Number of bytes per pixel. This number is 1 for all
                     SERCAA imager sensor data.

Image file data are stored in Tagged Image File Format (TIF), therefore an alternative way to determine image dimensions is to read the TIF header and examine the width and height fields.

Image pixel values represent retrieved property values. Cloud top effective altitude values are in the range 0-255 with 1 and 255 reserved for missing data. Cloud top effective pressure and emissivity values are in the range 0-100. Pressure units are 0.1 mb, emissivity are $\varepsilon * 100$. Table A-4 summarizes the attributes of the SOP data values.

Table A-4. SOP Output Products

Satellite ID	Product Name	Scale
N14 or N12 or GO8	altitude	1/17 km
	3.7 μm emissivity	$\varepsilon(*100)$
	10.5 μm emissivity	$\varepsilon(*100)$
	pressure	mb *10

Level 1:   **Latitude-Longitude File**

Latitude-longitude filenames as they appear on tape have the following naming convention:

YYDDHHMMEEE(EE).LAT
YYDDHHMMEEE(EE).LON

where

LAT - a constant that identifies the file as a latitude file
LON - a constant that identifies the file as a longitude file

48

YY - year of the satellite data for which the Earth locations are valid
DDD - Julian day of satellite data for which the Earth locations are valid
HH MM - UTC of the satellite data for which the Earth locations are valid
EEE(EE) - AIMS database entry number for the satellite data

File and Record Structure

Latitude-longitude Earth location files contain fixed-length records, the number and size of which depend on both the size of the corresponding image files and the satellite type. There is always one latitude-longitude record corresponding to each satellite image file record, where a satellite image file record contains one image scan line of information. There is one latitude-longitude pair for every image pixel.

A latitude-longitude file data element is a 2-byte structure that contains the scaled latitude or longitude for a given pixel. The storage convention is as follows:

LONG	Pixel longitude * 100. To obtain the floating-point longitude, FLONG = LONG / 100. Longitude range is -180° to 180°, positive east.
LAT	Pixel latitude * 100. to obtain floating-point latitude, FLAT = LAT / 100. Latitude range is -90° to 90°, positive north.

A-5.0 Data Extraction Guide

SOP product files use a standard naming convention as a means for identifying individual products. The convention for each product is as follows:

File Name	Description
yydddhhmmeeee.alt	TIF cloud-top altitude file
yydddhhmmeeee.e10	TIF 10 μm emissivity
yydddhhmmeeee.e37	TIF 3.7 μm emissivity
yydddhhmmeeee.prs	TIF cloud-top pressure
yydddhhmmeeee.lat	latitude for each pixel
yydddhhmmeeee.lon	longitude for each pixel

To correlate a file with other data from the same case, the file name encodes date and time where: yy represents the year, ddd the Julian day, hh the hour in UTC, mm the minute in UTC, and eeee a unique SDB entry number assigned to each scan. For example a file name of *95237011152264.prs* contains the cloud top pressure information for the data valid at 0115 UTC on day 237 of 1995. All other related product files (e.g., cloud-top altitude, emissivity, latitude, longitude) will share the entry number of 2264.

After reading the TIF data, to get the location of the pixel at row i, col j retrieve element i*row length + j from the latitude and longitude files. Calculations are zero relative.

Altitude values are stored in units of 1/17 km. (0-255 is Linear 0-15 km)
Pressure values are mb*10 (e.g., 63 = 630 mb)
Emissivity values are e*100 (21 = .21)

Altitude values 1 and 255 are reserved for missing data.

A-6.0 References

Gustafson, G.B., R.G. Isaacs, R.P. d'Entremont, J.M. Sparrow, T.M. Hamill, C. Grassotti, D.W. Johnson, C.P. Sarkisian, D.C. Peduzzi, B.T. Pearson, V.D. Jakabhazy, J.S. Belfiore, and A.S. Lisa, 1994: Support of Environmental Requirements for Cloud Analysis and Archive (SERCAA): algorithm descriptions. PL-TR-94-2114, Phillips Laboratory, Hanscom AFB, MA, ADA283240.

Hoke, J.E., J.L. Hayes, L.G. Renninger, 1981: Map projections and grid systems for meteorological applications. AFGWC-TN-79-003, Air Weather Service, Scott AFB, IL.